Carla Sofia Gomes Ferreira

# Is endothelial dysfunction the one to blame in Heart Failure with Preserved Ejection Fraction?

Dissertation for Master Degree in Biomedical Research

July, 2015

· U C ·

UNIVERSIDADE DE COIMBRA

Carla Sofia Gomes Ferreira

# Is endothelial dysfunction the one to blame in Heart Failure with preserved Ejection Fraction?

Dissertation presented to the Faculty of Medicine of the University of Coimbra for the fulfillment of the requirements for a Master degree in Biomedical Research

Dissertação apresentada à Faculdade de Medicina da Universidade de Coimbra para prestação de provas de Mestrado em Investigação Biomédica

July, 2015

UNIVERSIDADE DE COIMBRA

## Host Institution


Departamento de Fisiologia e Cirurgia Cardiotorácica
Cardiovascular R&D Unit
Centro de Investigação Médica, 6º piso
Faculdade de Medicina da Universidade do Porto
Rua Dr Plácido da Costa
4200-450 Porto, Portugal

**Supervisor:** Inês Falcão-Pires, PhD[1]

**Co-supervisor:** Henrique Girão, PhD[2]

**Affiliations:**

[1] FMUP - Faculdade de Medicina da Universidade do Porto

[2] FMUC - Faculdade de Medicina da Universidade de Coimbra

## Acknowledgements

My Master thesis was an extraordinary journey. I feel a very lucky person! I met wonderful people and I would like to express my profound gratitude:

To Professor Adelino Leite-Moreira, head of the Department of Physiology and Cardiothoracic Surgery, for having received me in your laboratory, for giving me the opportunity to work with your big team and for being so nice to me. I will never forget that, like you said, “I have an additional responsibility”!

To Professora Inês, my supervisor, for giving me the opportunity to work with you and your team and for your scientific guidance. I hope to continue to be part of your time.

To Professor Henrique, for being my “father” in Coimbra, for your attention and for all the wisdom.

To Doutora Diana Nascimento, from helping me to understand flow cytometry and for all the help with endothelial cells.

To Nádia for helping me growing, for helping me to understand my thesis! You teach me all I know about HFpEF and genetics! Thank you for almost being my co-supervisor. Because of you genetic is no more a “black hole” in my life. Thank so much you for the advices, your patience, kindness and for making me feel “like home”.

To Glória, for being my teacher, my tutor in FMUP, for all your patience, kindness and friendship.

To Ana for helping me growing, for all advices and for have left me stay in your office for so long! Thank you for always comforted me when I needed and thank you for, like Nádia, making me feel “like home”.

To Daniela, Patrícia, Dulce and João, from my group, for all the help with the results and with the writing of my thesis.

To Paulo, for being a friend that always make me smile with your jokes, to Sara for teaching me Medicine and for all advices and Manuel.

To all Cardiovascular R&D Unit family, that was been my family work for almost one year and half.

Ao meu melhor amigo e namorado, João, por acreditar em mim e por estar sempre lá quando eu precisei.

Às pessoas mais importantes da minha vida, a minha mãe e o meu pai, por me terem dado a oportunidade de ser Mestre e por sempre acreditarem em mim.

*Carla Sofia Gomes Ferreira*

## Abstract

Heart Failure with preserved Ejection Fraction (HFpEF) is a common clinical syndrome that comprises 50% of Heart Failure (HF) patients. It is characterized by an abnormal diastolic left ventricular (LV) function, with impaired relaxation and increased stiffness that together contribute to the heart inability to fill properly. Understanding HFpEF has been difficult due to its heterogeneous etiology and pathophysiology, so, treatment options are still an enigma. Recent studies on HFpEF emphasize the importance of comorbidities frequently present in this syndrome, like diabetes mellitus (DM), obesity, hypertension and even aging, all promoting systemic inflammation and endothelial dysfunction.

The recently characterize ZSF1 obese rat represents one of the most comprehensive animal model of HFpEF described to date. Using this model, we aim to better characterize HFpEF in terms of assessing inflammation, endothelial function and the relation between these injuries, allowing for a better understanding of this syndrome.

Male rats Wistar Kyoto (WKY, n=21), ZSF1 Lean (ZSF1Ln, n=24) and ZSF1 Obese (ZSF1Ob, n=22) were subjected to echocardiographic examination at their 18$^{th}$ week of age and, at the end of the protocol, to morphometric and vascular function evaluation, as well as molecular and histological studies.

Compared to WKY and to ZSF1Ln, ZSF1Ob rats are heavier, present obesity with significantly more abdominal adiposity, other features of DM and also hypertension, three important risk factors for HFpEF. ZSF1Ob animals have LV hypertrophied and display diastolic dysfunction, in which an increase in E/E' was observed. Aortic rings, submitted to acetylcholine increasing concentrations, showed endothelium impairment of relaxation, suggesting endothelial dysfunction. ZSF1Ob animals do not presented systemic inflammation but had myocardial expression of inflammatory mediators, revealing itself to be the principal source of heart tissue inflammation.

We conclude that ZSF1Ob rat represent a solid animal model for HFpEF research and that cardiac endothelium underlies its pathophysiology thus representing an interesting pathway for future pharmacologic interventions.

**Keywords:** Heart Failure with preserved Ejection Fraction; inflammation; endothelial dysfunction; ZSF1 obese animal model

## Resumo

Insuficiência cardíaca com fração de ejeção preservada (ICFEP) é um síndrome clínico bastante comum que compreende 50% dos doentes com insuficiência cardíaca (IC). A ICFEP é caracterizada por uma função ventricular comprometida, nomeadamente com alterações no relaxamento e aumento da rigidez, que em conjunto contribuem para a incapacidade do coração de encher de maneira eficiente. Compreender a ICFEP tem sido difícil devido à sua etiologia e patofisiologia heterogéneas, o que limita as opções de tratamento. Descobertas recentes dão ênfase às comorbilidades frequentemente presentes na ICFEP, como a diabetes mellitus, obesidade e hipertensão e até mesmo o envelhecimento, como sendo promotoras de inflamação sistémica e disfunção endotelial.

O rato obeso ZSF1 recentemente caracterizado representa um dos melhores modelos animais para a investigação na ICFEP. Utilizando este modelo pretendemos avaliar a inflamação e a disfunção endotelial e ainda a relação entre ambos, permitindo assim uma melhor compreensão deste síndrome.

Ratos machos com nove semanas de idade Wistar Kyoto (WKY, n=21), ZSF1 magros (ZSF1Ln, n=24) e ZSF1 obesos (ZSF1Ob, n=22) foram submetidos a avaliações ecocardiográficas às 18 semanas de idade, e no fim do protocolo, a avaliações morfométricas e de função vascular, assim como a estudos moleculares e histológicos.

Comparando com os grupos WKY e ZSF1Ln, os ratos ZSF1Ob têm mais peso corporal, são obesos e têm mais gordura abdominal, possuem características da diabetes mellitus e hipertensão, três fatores de risco relacionados com a ICFEP. Os ratos ZSF1Ob têm hipertrofia ventricular esquerda e apresentam disfunção diastólica, com um aumento da razão E/E'. Anéis aórticos submetidos a concentrações crescentes de acetilcolina mostraram um comprometimento no relaxamento do endotélio, sugerindo um estado de disfunção endotelial. Células endoteliais cardíacas de animais

ZSF1Ob mostraram expressão de factores inflamatórios importantes, revelando ser a principal fonte de inflamação no tecido cardíaco.

Conclui-se que os ratos ZSF1Ob representam um bom modelo animal para investigação na ICFEP e que o endotélio cardíaco é alvo interessante para futuras intervenções farmacológicas.

**Palavras-chave:** Insuficiência cardíaca com fração de ejeção preservada; inflamação; disfunção endotelial; modelo animal ZSF1 obeso

# List of contents

# Figure index

# Table index

## Abbreviations list

| | | |
|---|---|---|
| **Ach** | - | Acetylcholine |
| **AGEs** | - | Advanced Glycation End-products |
| **Ang II** | - | Angiotensin II |
| **Ang 1-7** | - | Angiotensin 1-7 |
| **BSA** | - | Body Surface Area |
| **cGMP** | - | cyclic Guanosine Monophosphate |
| **CI** | - | Cardiac Index |
| **CML** | - | Carboxymethllysine |
| **CO** | - | Cardiac Output |
| **COPD** | - | Chronic Obstructive Pulmonary Disease |
| **DM** | - | Diabetes Mellitus |
| **EDVI** | - | End-diastolic volume index |
| **EF** | - | Ejection Fraction |
| **ESVI** | - | End-systolic volume index |
| **ET-1** | - | Endothelin-1 |
| **eNOS** | - | endothelial Nitric Oxide Synthase |
| **FABP4** | - | Fatty Acid Binding Protein 4 |
| **FS** | - | Fractional Shortening |
| **GAPDH** | - | Glyceraldehyde 3-phosphate dehydrogenase |
| **HF** | - | Heart Failure |
| **HFrEF** | - | Heart Failure with reduced Ejection Fraction |
| **HFpEF** | - | Heart Failure with preserved Ejection Fraction |
| **HR** | - | Heart Rate |
| **ICAM1** | - | Intracellular Adhesion Molecule 1 |
| **Il-1** | - | Interleukin-1 |
| **Il-6** | - | Interleukin-6 |
| **Il-8** | - | Interleukin-8 |
| **IR** | - | Insulin Resistance |
| **LAA** | - | Left Atrium Area |
| **LV** | - | Left Ventricle |

| | | |
|---|---|---|
| **MCP1** | - | Monocyte Chemoattractant Protein 1 |
| **MPI** | - | Myocardial performance index |
| **NF-Kβ** | - | Nuclear Factor – kappa β |
| **NO** | - | Nitric Oxide |
| **NOX2** | - | NADPH oxidase 2 |
| **NOX4** | - | NADPH oxidase 4 |
| **Phe** | - | Phenylephrine |
| **PKG** | - | Protein Kinase G |
| **RAGE** | - | receptor of Advanced Glycation End-product |
| **RANTES** | - | Regulated on activation normal T cell expressed and secreted |
| **ROS** | - | Reactive Oxygen Species |
| **RV** | - | Right Ventricle |
| **sGC** | - | soluble Guanylate Cyclase |
| **SHHF** | - | Spontaneously Hypertensive Heart Failure |
| **SV** | - | Stroke Volume |
| **S'** | - | Mitral annular systolic velocity |
| **TGFβ** | - | Transforming Growth Factor β |
| **TNFα** | - | Tumor Necrosis Factor α |
| **VASP** | - | Vasodilator-stimulated Phosphoprotein |
| **VCAM1** | - | Vascular Adhesion Molecule 1 |
| **WKY** | - | Wistar Kyoto |
| **ZSF** | - | Zucker Fatty/ Spontaneously Hypertensive Heart Failure F1 hybrid rats |

# Part 1

## Introduction

*“There are many hypotheses in science which are wrong. That’s perfectly all right: it’s the aperture to finding out what’s right. Science is a self-correcting process.”*

Carl Sagan

# 1. Heart Failure

## 1.1. Definition

The first description of Heart Failure (HF) remotes to ancient Egypt times. Its definition remains controversial partly because of his complicated etiology and also because of the variability of the clinical symptoms and signs. HF is the end-result of many cardiovascular diseases and a clinical syndrome characterized by functional and structural irregularities in human heart that compromise its capacity to eject sufficient blood to fulfill all body's metabolic needs or only at the expense of increased ventricular filling pressures [1-3].

## 1.2. Epidemiology

The epidemiology of HF had a remarkable revolution in the last decades. Worldwide the total number of estimated HF patients is around 26 million. Results from the Framingham Heart Study suggest that in developed countries, at some point of their life, one in five persons will develop HF. In Europe, according to the Rotterdam study, the 5-year mortality risk is around 41% [4, 5].

The number of patients with HF will grow to epidemic proportions considering the expected increase of population ageing, the sedentary lifestyle expected for the next years and the estimated increase of HF comorbidities like diabetes mellitus (DM) and obesity, thus representing a major public health problem [4-6].

### 1.3. Symptoms and signs

According to European Society of Cardiology, symptoms of HF include dyspnea (difficulty in breathing), fatigue and exercise intolerance [7, 8].

Signs of HF include leg, ankles and feet swelling, jugular distension, pulmonary rales, peripheral edema and some radiographic manifestations like pulmonary vascular redistribution, interstitial edema and pleural effusions [8].

### 1.4. Classification and Pathophysiology

According to the European Society of Cardiology and to the American College of Cardiology Foundation/American Heart Association HF patients can be divided in two clinically distinct syndromes: HF with reduced Ejection Fraction (HFrEF) or systolic HF and HF with preserved Ejection Fraction (HFpEF) also known as diastolic HF [9].

HFrEF is correlated with ischemic injury, dilated and other genetic cardiomyopathies, whereas HFpEF is associated with chronic inflammation and the co-existence of other comorbidities which represent important cardiovascular risk factors. Comparing both types, HFpEF patients have fewer hospitalizations but higher mortality rate than HFrEF. Contrarily to HFrEF, there is not any effective medical treatment for HFpEF as a result of the diversity and complexity of pathophysiology of this condition [7, 10]. The heterogeneous etiologies and the challenging diagnostic make HFpEF an interesting topic for research. Current treatment strategies focus on control of volume status and comorbidities, but future research aimed at individualized therapies holds promise to improve outcomes in this increasingly prevalent form of cardiac failure.

### *1.4.1. Heart Failure with Preserved Ejection Fraction*

HFpEF constitutes almost 50% of all HF patients and its prevalence is increasing almost 1% per year [11]. HFpEF is more common in older women (61-76% of patients) with high prevalence of hypertension, DM, ischemic heart disease, coronary artery disease, atrial fibrillation and lifestyle related risk factors like smoking and obesity [1, 12-16].

HFpEF is associated with left ventricle (LV) diastolic dysfunction and involves complex interactions between multiple factors. In the diastolic phase, the ventricle is unable to fill with sufficient blood maintaining adequate low pressures resulting from myocardium stiffness or impaired relaxation. The increased filling pressure (stiffness) induces wall thickness and an adjustment in ventricular size and volume (Figure 1) [8, 17-20]. Besides the diastolic dysfunction, some other mechanisms seem to be related with HFpEF pathophysiology, such as inflammation, chronic volume overload, venous constriction, irregular ventricular-vascular coupling, as well as cardiac autonomic impairment and chronotropic incompetence. In this condition the heart rate response to stress is abnormal what could lead to pulmonary arterial hypertension and endothelial dysfunction [15].

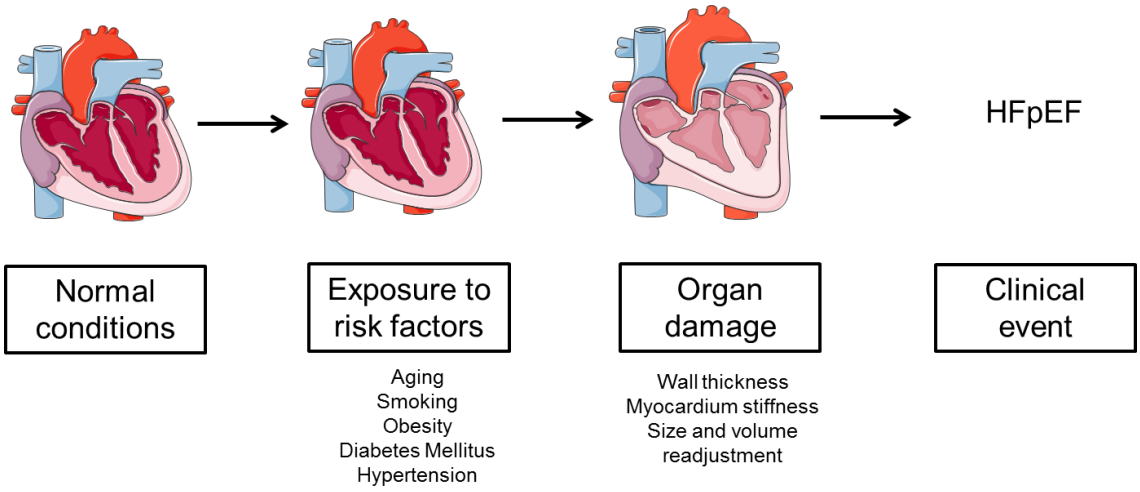


**Figure 1.** Schematic representation of the evolution of a normal heart into HFpEF, involving the exposure to several risk factors. Risk factors are responsible for myocardium alterations that include readjustment in ventricular size and volume, myocardium stiffness and wall thickness, therefore contributing to the development of HFpEF. Figure was produced using Servier Medical Art.

The challenging diagnosis of HFpEF is assessed after clinical evaluation, Doppler echocardiography or invasive hemodynamic assessment and confirmed whenever the following conditions are observed [7, 21, 22]:

- Signs and symptoms of HF;
- Diastolic dysfunction;
- Normal or lightly anomalous systolic function.

Despite all advances in medicine, HFpEF continues to have a high rate of hospitalizations, subsequent readmission on hospital, a considerable mortality rate (10-30%) and will grow to epidemic proportions making it a major public health problem [1, 12, 23].

### 1.5. Comorbidities in HFpEF

Non-cardiac comorbidities are highly prevalent in HFpEF and have an important role in the pathogenesis of this syndrome [11]. Several risk factors are involved, although only one is enough to cause HFpEF. Patients with HFpEF usually have multiple comorbidities that could cause or be contributors to this phenotype [15].

Female gender is also an important risk factor being associated with more concentric remodeling, lower LV diastolic volumes and as well as systolic and diastolic LV stiffness. Woman have a probability two times higher to develop HFpEF [11, 24].

Anemia is present in 50-70% of HFpEF patients and it is closely related with renal disease and it is characterized by iron deficiency and insufficient erythropoietin production generated by systemic inflammation. Chronic renal failure and HFpEF often co-exist and share common risk factors. Indeed, renal failure is present in 30-40% of patients and it is a predictor of mortality. Chronic obstructive pulmonary disease (COPD) also contributes to HFpEF

mortality and the adverse cardiovascular effects include reduction of cardiac output, less stroke volume and also impaired LV filling [11, 25].

Hypertension is the most predominant risk factor, being present in 60-88% of HFpEF patients. In hypertensive patients, the risk of developing HFpEF is 2 times higher in men and 3 times higher in women comparing with the normotensive patients. High blood pressure is capable of increase arterial stiffness, which compromises LV relaxation. Additionally, these patients frequently display obesity, microalbuminuria and impairment of insulin signaling and rapidly develop myocardial fibrosis and LV hypertrophy [11].

Obesity, which has reached epidemic proportions partly because of the increase of energy intake and a sedentary life style, impairs cardiac structure and function that doubles the risk of having HFpEF. It is present in 32-46% of patients and it is an independent risk factor for cardiovascular morbidity and mortality. Along with adipose tissue expansion, pro-inflammatory cytokines and adipokines, like leptin and resistin, are released. Arterial resistance increases and contributes to LV hypertrophy and high diastolic pressures. Myocardial relaxation is compromised due to changes in cardiomyocyte calcium handling, along with lipotoxicity and mitochondrial dysfunction. All these alterations induce LV concentric remodeling, LV increase of mass e volume and arterial stiffness [11, 12].

Diabetes mellitus (DM) is a recognized comorbidity affecting 30-45% of HFpEF patients, especially females. The Framingham Heart Study first showed that diabetic patients can develop diastolic LV thickness with stiffer cardiomyocytes and subsequent studies from our group further confirmed this evidence [26]. This is a result of hyperglycemia effects that causes interstitial and perivascular fibrosis, increase collagen deposition and reduction of degrading matrix metalloproteinases [11, 12, 15]. Additionally, high levels of glucose promote the generation of advanced glycation end-products (AGEs) in myocardium, which are molecules formed in the reducing sugars' reaction that can form covalent bonds with proteins, namely collagen fibers cross-linking, stiffening the myocardium. Moreover, AGEs can bind their receptors,

RAGEs, increasing collagen production thus, decreasing arteries distensibility and increasing LV stiffness [11, 27, 28].

All the previous comorbidities are associated with several pathological changes in the cardiovascular system that strongly contribute to HFpEF. Besides diastolic LV dysfunction, myocardial and systemic inflammation, oxidative stress and endothelial dysfunction represent important contributors to the pathophysiological mechanisms of HFpEF syndrome [11, 12]. The endothelium, located between the circulating blood and the vessel wall or the myocardium, occupies a strategic anatomic position and is undoubtedly involved in the abnormalities that occur in HFpEF [29-34].

# 2. HFpEF and the endothelium

## 2.1. The endothelium

Endothelium is an active organ formed by a monolayer of endothelial cells that separate the vascular wall or the myocardium from the circulation. It acts as a functional and structural barrier capable of sensing hormonal and mechanical stimuli. The endothelium plays an important role in cardiovascular homeostasis modulating vascular tone by balancing the production of vasodilators and vasoconstrictors agents (Table 1). In addition, this layer also regulates solute transport, prevent leucocyte and platelet adhesion and aggregation, modulates blood flow and mediates inflammatory and reparative response to injury [32, 35-37]. Cardiac endothelium integrates endothelial cells from endocardium, from the coronary microvasculature and also of the intramyocardial capillaries. The anatomical position of endothelial cells next to cardiomyocytes enables a bidirectional communication between those cells [38]. Several studies have shown that endothelium have a crucial role in several diseases, including HFpEF [35, 39].

**Table 1.** Vasoactive and inflammatory substances released by endothelium [36, 40].

| Action | Substance |
|---|---|
| Vasodilation | Nitric Oxide (NO)<br>Prostacyclin<br>C-Type natriuretic peptide |
| Vasoconstriction | Endothelin-1 (ET-1)<br>Angiotensin II (Ang II)<br>Thromboxane $A_2$<br>Reactive Oxygen Species (ROS) |
| Inflammation | Nitric Oxide (NO)<br>E and P-selectin<br>Nuclear Factor kβ (NF- kβ)<br>ICAM1<br>VCAM1 |

Nitric oxide (NO) is the most important and the most characterized substance produced by the endothelium. This gas with a short life (about 6-30 seconds) is generated from L-arginine amino acid by endothelial NO synthase (eNOS) which is continuously produced and release by endothelial cells through physical and hormonal stimuli [41]. Shear stress caused by blood flowing on the vessel wall is the most important physical stimuli for NO production. Chemical stimuli include acetylcholine, bradykinin and serotonin [41, 42]. In the healthy endothelium, when NO is released, binds to smooth muscle promoting the activation of soluble Guanylate Cyclase (sGC) and the production of cyclic Guanosine Monophosphate (cGMP) which opens calcium dependent potassium channels promoting blood vessel relaxation and vasodilation (Figure 2). Normally, NO is important to maintain the vascular wall in a quiescent state inhibiting inflammation, cell proliferation and thrombosis being the vasodilation prevalent (Table 2) [41-45].

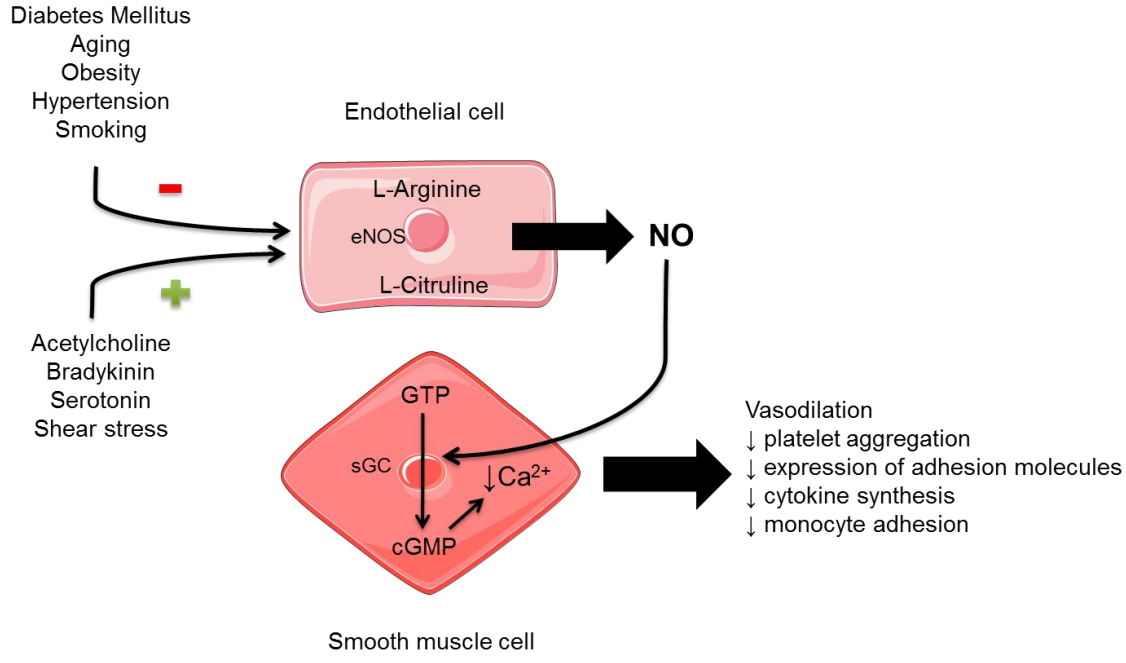


**Figure 2.** Synthesis of Nitric Oxide. In endothelial cells NO production is stimulated by several stimulus and inhibited by others. NO acts in smooth muscle cells in order to promote vasodilation and the decrease of cytokine synthesis, the monocyte adhesion and platelet aggregation, as well as the decrease of adhesion molecules. NO: Nitric Oxide; eNOS: endothelial Nitric Oxide Synthase; GTP: Guanosine Triphosphate; sGC: soluble Guanylate Cyclase; cGMP: cyclic Guanosine Monophosphate. Figure was produced using Servier Medical Art. Adapted from [41, 42].

**Table 2.** Role of Nitric Oxide. Adapted from [41].

| Role | Action |
|---|---|
| Vasomotor action | Endothelium vasodilation<br>Decreases vasoconstriction in smooth muscle cells<br>Regulation of systemic and coronary tone by acting on basal arterioles |
| Inflammation | Decreases endothelial permeability<br>Decreases expression of E-selectin<br>Reduction of leucocyte adherence to the endothelium<br>Decreases production of macrophages cytokines<br>Down-regulate platelet aggregation and adherence |
| Antioxidant | *In vivo* and *in vitro* free radical scavenger<br>NO donors duplicate plasma anti-oxidant capacity |

### 2.2. Endothelial dysfunction

As a consequence of HFpEF risk factors, endothelium loses his integrity and the homeostatic balance is disrupted, culminating in endothelial dysfunction. Endothelium acquires a pro-inflammatory and pro-thrombotic state with vasoconstriction that includes detachment and release of endothelial cells into the circulation [35, 39, 44, 46]. Endothelial dysfunction is associated with the beginning and the progression of HFpEF [32, 34, 40, 47].

The principal feature of endothelial dysfunction is the impairment of NO bioavailability. In this condition, reduced production of NO can result from diverse contributing factors, such as decreased production of eNOS, lack of eNOS substrates or due NO degradation by ROS (Figure 3). ROS are chemical oxygen species and cellular metabolism's products that are highly reactive causing oxidative stress [37, 38]. ROS form peroxinitrites that impair the NO-induced vasodilation, essential to vascular homeostasis and

endothelial function. Reduced NO release by endothelium affects ventricular relaxation, particularly in the hypertrophied myocardium. Conventional antioxidant therapies have intended to correct the imbalance between NO and ROS, but sadly have not been totally successful yet [36, 40, 48-50].

The link between endothelial dysfunction and HFpEF pathophysiology is currently established [11, 32, 33, 36, 41]. However the precise mechanisms remain obscure. Understanding endothelial dysfunction mechanisms will be an important key to understand the pathophysiology of HFpEF.

A – Normal endothelium

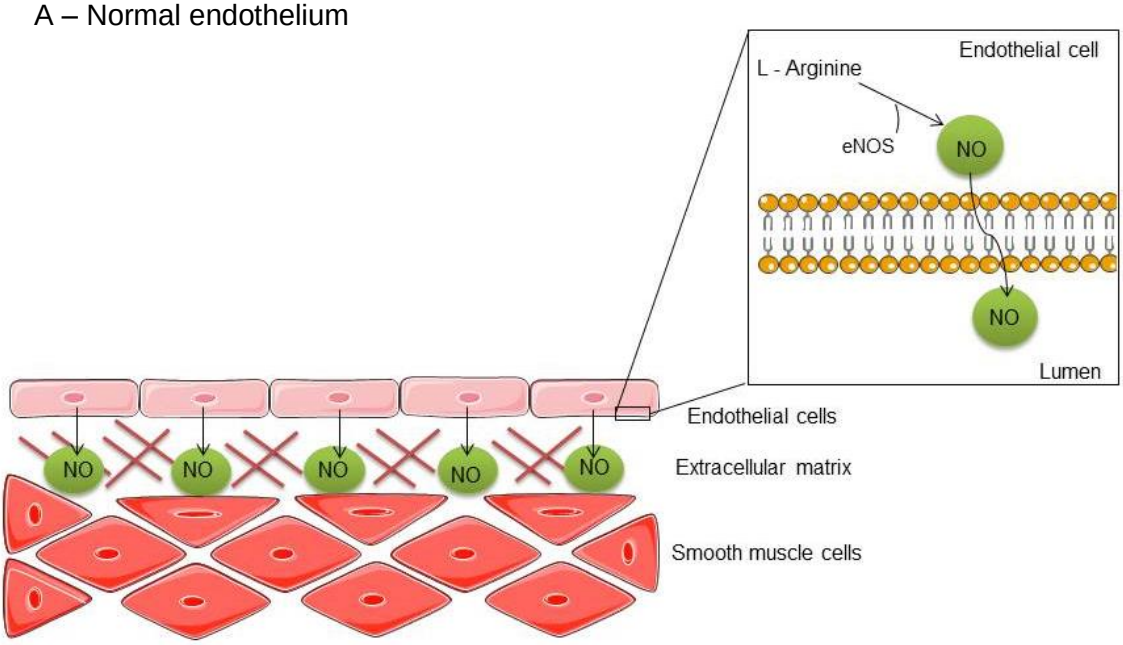


B – Dysfunctional endothelium

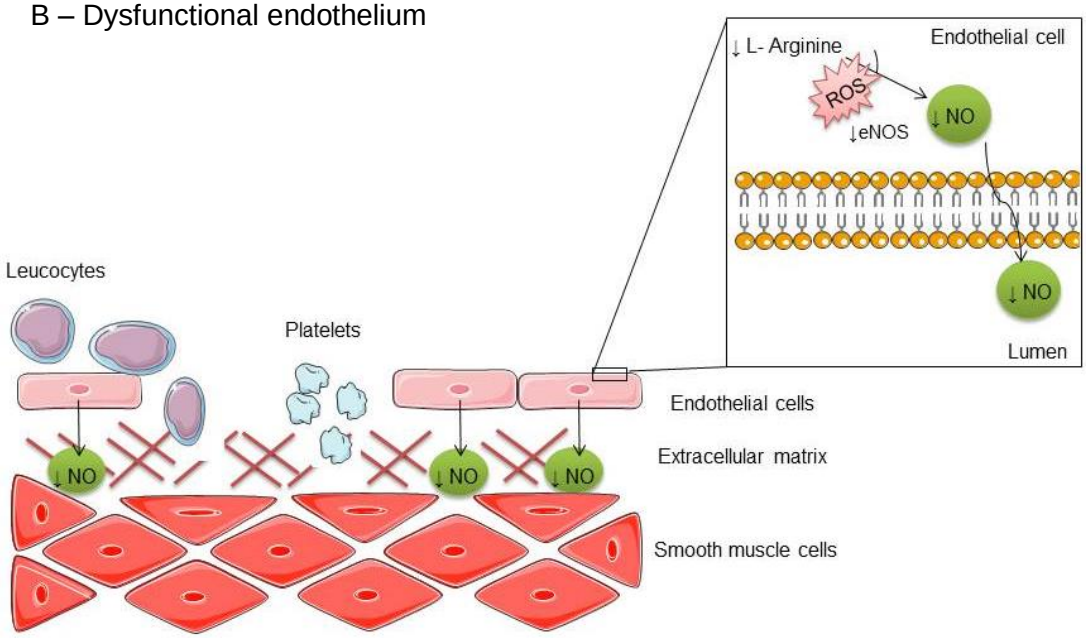


**Figure 3.** Schematic representation of the differences between a healthy (A) and dysfunctional endothelium (B). In a healthy endothelium, endothelial cells are intact and produce a normal concentration of nitric oxide (NO) by endothelial nitric oxide synthase (eNOS). In a dysfunctional endothelium, endothelial cells are damaged and produce a reduced concentration of NO due reaction with reactive oxygen species (ROS) and a decreased eNOS activity. It becomes an inflammatory local and leucocytes and platelets migrate to this injury site. Figure was produced using Servier Medical Art.

## 2.3. Mechanisms of endothelial dysfunction in HFpEF: the role of comorbidities

Newer insights suggest that endothelial dysfunction is more than a state of systemic vasoconstriction and that has a crucial role in HFpEF pathogenesis. In 2013 Paulus *et al*. suggested that endothelial dysfunction plays a central role in HFpEF progression. These new paradigm of HFpEF suggests that comorbidities are responsible for the pro-inflammatory state seen, causing coronary microvascular endothelial inflammation [51].

Hypertension, obesity and DM induce a systemic inflammatory state with the release of pro-inflammatory cytokines such as tumor necrosis factor α (TNFα), interleukin-1 (Il1), Il-6 and Il-8. Increased circulating levels of these cytokines are found in HFpEF patients [11, 13]. The adhesion molecules, vascular cell adhesion molecule 1 (VCAM1), intercellular adhesion molecule 1 (ICAM1) and E-selectin, which in normal conditions are expressed in small amounts in the surface of endothelial cells, are upregulated [13, 52]. Endothelial inflammation originates the production of ROS that leads to peroxynitrites ($ONOO^-$) formation and a decrease in NO bioavailability. In response, cardiomyocyte production of soluble guanylate cyclase (sGC) is reduced, which contributes to a decrease in cGMP and protein kinase G (PKG) concentration. In HFpEF lower PKG levels are associated with cardiomyocyte hypertrophy and stiffness, and with high resting tension ($F_{passive}$). This high resting tension is due to the hypophosphorylation of the N2B segment of the giant cardiomyocyte cytoskeletal protein titin [11, 38, 51, 53]. Microvascular endothelial inflammation also stimulates fibroblasts differentiation in myofibroblasts resulting in myocardial fibrosis with collagen type 1 deposition and collagen cross-linking, which are contributors to myocardial stiffening [54]. These changes induce diastolic LV dysfunction, the major characteristic of HFpEF (Figure 4) [11, 38, 51].

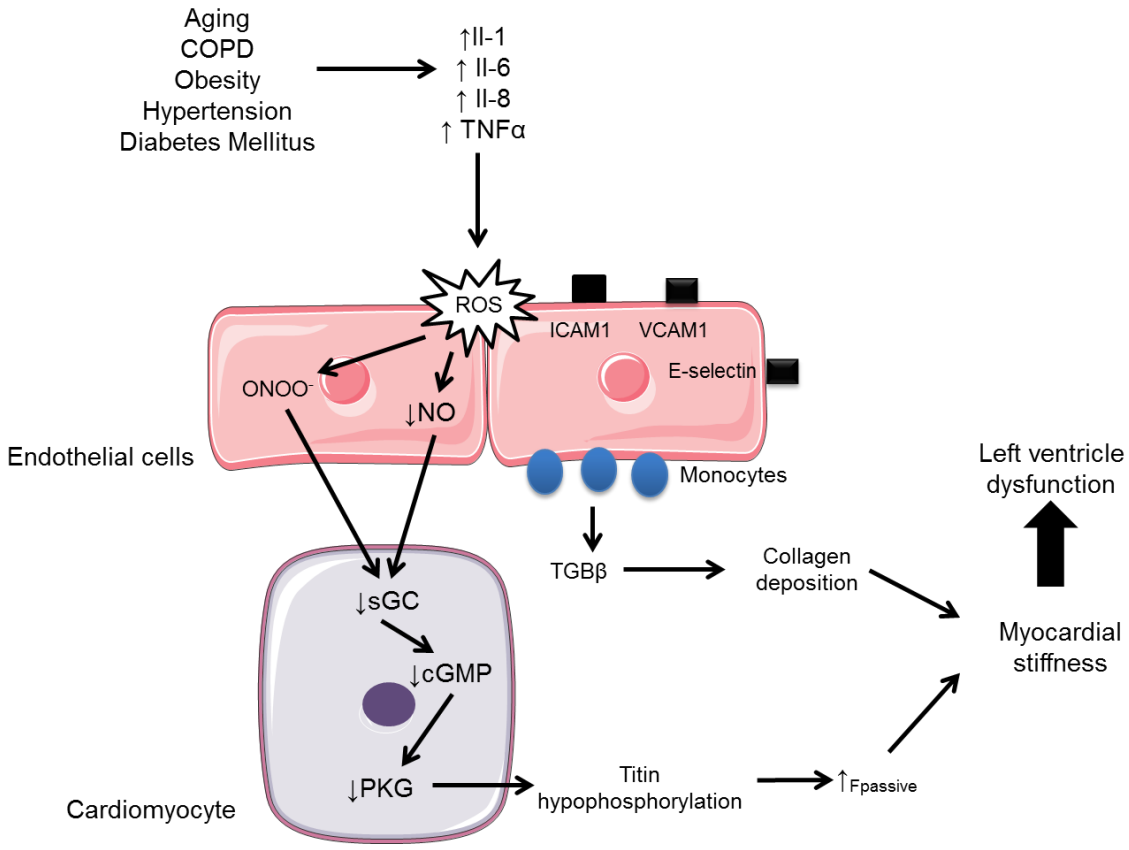


**Figure 4.** Schematic representation of the mechanisms induced by comorbidities that result in myocardial dysfunction and remodeling in HFpEF. Comorbidities generate a pro-inflammatory state with consequent release of Interleukin (Il) 1, Il-6, Il-8 and Tumor Necrosis Factor α (TNFα). Endothelium produces reactive oxygen species (ROS) that react with nitric oxide (NO) to produce peroxynitrites ($ONOO^-$) and at the same time reduce NO bioavailability. In cardiomyocytes there is a reduction in soluble guanylate cyclase (sGC), which in turn decreases cyclic guanosine monophosphate (cGMP) concentration and protein kinase G (PKG) production. Titin hypophosphorylation induces an increase in passive force leading to cardiomyocyte hypertrophy. Endothelial cells increase the expression of adhesion molecules (ICAM1, VCAM1 and E-selectin) influencing the migration of monocytes that release transforming growth factor (TGFβ). This last induces the collagen production and deposition in interstitial space which is turn causes cardiomyocyte stiffness. Figure was produced using Servier Medical Art. Adapted from [11, 51].

Nevertheless, the exact role that comorbidities have on structural and functional remodeling in HFpEF is not entirely well known. The new paradigm of HFpEF could be a new therapeutic target and the development of experimental HFpEF models might be beneficial and helpful, in order to understand and possibly to cure this pathology [11].

# 3. Animal models in HFpEF research

Understanding the pathophysiology of HFpEF has been restricted by the limited access to human myocardial biopsied due to obvious ethical constrictions. In addition, the lack of a proper animal model mimicking the human pathology has partly limited HFpEF research. Indeed, animal models can be very useful to clarify subcellular mechanisms under conditions where the comorbidities and other confounding factors can be precisely controlled [55, 56].

There are several models used for HFpEF research, nevertheless, until recently, none had fulfilled all the features present in the human disease. Recently, we have characterized a rat model that meets the criteria of HFpEF, the obese ZSF1 [57].

## 3.1. The obese ZSF1 as an animal model of HFpEF

ZSF1 rats were generated by crossing non-hypertensive lean female Zucker Diabetic Fatty rats (ZDF, +/fa) with lean spontaneously hypertensive HF prone male rats (SHHF/Mcc, +/fa$^{cp}$) that share a common genetic background with Wistar Kyoto (WKY) rats and derive from spontaneously multifactorial hypertensive rats [58-63]. Both lean and obese ZSF1 animals, inherit a hypertensive gene from the spontaneously hypertensive rat strain and show elevated blood pressure [59].

ZSF1 rats have myocardial hypertrophy induced by hypertension, more notorious in obese than in lean rats. The ZSF1 obese rats present considerable diastolic abnormalities such as increased left atrial area, prolonged time constant of isovolumetric relaxation, elevated arterial elastance and end-diastolic pressure as well as an upwards shift of end-diastolic pressure-volume relation, thus highlighting a worse ventricular-vascular coupling. Systolic function remained preserved in lean and obese ZSF1 rats [57].

In terms of metabolic disturbances, ZSF1 obese animals developed obesity, abdominal adiposity, insulin resistance, oral glucose intolerance, hyperglycemia and glycosuria, consistent with type II DM phenotype [64] and thus represent a good animal model of metabolic syndrome. Moreover, compared to hypertensive ZSF1 lean, which represent a model of isolated ventricular overload, the ZSF1 obese will allow clarifying if imposing metabolic comorbidities on top of overload is per se capable of induced HFpEF. Recently, a full description of a rat model that meets the criteria of diastolic HF was described, the ZSF1 obese [57].

# Part 2

## Aims

*‘‘The scientist is not a person who gives the right answers; he's one who asks the right questions.”*

Claude Lévi-Strauss

Considering the concepts reviewed before, the aim of the present study was to clarify the pathophysiology of HFpEF by investigating the contribution of endothelial dysfunction and inflammation for the development of this syndrome.

In order to achieve the aim of the project we pretend to:

- Characterize an animal model of HFpEF including metabolic, morphometric as well as cardiac structural and functional changes;
- Evaluate endothelial dysfunction in the previous model;
- Correlate endothelial dysfunction with cardiac function parameters to investigate potential therapeutic targets.

# Part 3

## Materials and Methods

*"Those who are quite satisfied sit still and do nothing; those who are not quite satisfied are the sole benefactors of the world."*

Walter Savage Landor

## 1. Experimental animal model

This study was made according to the Guide for the Care and Use of Laboratory Animals published by the NIH (NIH Publication no. 85–23, revised 2011) and was approved by the ethics committee of the Faculty of Medicine of Porto and by Direção-Geral de Alimentação e Veterinária (DGAV) from Portugal. The Faculty of Medicine of Porto is a governmental institution, granted approval by the Portuguese government to perform animal experiments.

Nine-weeks old male rats Wistar Kyoto (WKY, n=21), ZSF1 Lean (ZSF1Ln, n=24) and ZSF1 Obese (ZSF1Ob, n=22) were obtained from Charles River (Barcelona, Spain) and had unlimited access to food (LabDiet® 5008, International Product Supplies Ltd., UK) and water. Animals were housed in groups of 2 animals per cage in a ventilated cages system (IVC) in a controlled environment with a 12-h-light/-dark cycle at 22ºC room temperature. The room had a relative humidity of 30–70% and an air exchange rate of 40–50 air changes/hour.

In the end of the experiment, at their 20$^{th}$ week of age, anesthetized animals (8% for induction and 2.5-3% for maintenance) were euthanized by exsanguination and blood and tissue were collected. Organs were weighed, RV and LV were weighed after dissection, and tibia length (TL) was measured. Fresh samples of LV were used in flow cytometry and the rest of the samples were snap-frozen in liquid nitrogen and stored at -80ºC for molecular studies (RNA extraction, western blot) or fixed in 10% buffered formalin for histological procedures and also for immunohistochemistry analysis. Weights were normalized to TL due to the large body weight differences between groups.

## 2. Echocardiography

All animals were subjected to an echocardiography evaluation at their 18$^{th}$ week. Animals were anaesthetized by inhalation of sevoflurane (8% for induction and 1-2.5% for maintenance), orotracheally intubated and mechanically ventilated (150 $min^{-1}$, 100% $O_2$, 14–16cm$H_2O$ inspiratory pressure, with tidal volume adjusted to animal weight, and 4cm$H_2O$ end-expiratory pressure) (TOPO Small Animal Ventilator, Kent Scientific Inc., USA). Rats were placed in a left-lateral decubitus position on a heating pad, the ECG was monitored and their temperature was kept at 38ºC. The skin of all animals was shaved, the echocardiography gel was applied and a linear 15MHz probe (Sequoia 15L8W) was gently positioned on the thorax. Systolic and diastolic wall thickness and cavity dimensions were recorded, in M-mode and 2D echocardiography, at the level immediately above the papillary muscles in the parasternal short axis view.

From these measurements end diastolic and end systolic volumes, (EDV and ESV, respectively), fractional shortening (FS), ejection fraction (EF) of the LV, stroke volume (SV) and cardiac output (CO) were derived. The following Doppler and tissue Doppler measurements were taken using the apical four-chamber early diastolic filling peak velocity (E wave), late diastolic peak velocity (A wave), E/A ratio, early peak diastolic filling velocity (E'), late peak diastolic filling velocity (A') and mitral annular systolic velocity (S').

The myocardial performance or TEI index was retrieved from the mitral flow pattern and calculated by the formula = (IVCT + IVRT)/ET, were IVCT is the isovolumic contraction time, IVRT corresponds to the isovolumic relaxation time and ET to ejection time. Data was indexed for body surface area as described previously [65] and three representative cycles were measured per rat and their average was calculated.

## 3. ELISA assay

Blood samples collected from subclavian vein after echocardiographic evaluation were placed in tubes with EDTA ($C_{10}H_{16}N_2O_8$, pH 6.0). Samples were centrifuged at 5000 rpm for 15 minutes at 4°C and plasma was then separated and utilized for quantitative enzyme immunoassays (ELISA).

Levels of leptin (SK00050-08, Adipo bioscience, USA), Fatty Acid Binding Protein 4 (FABP4, SK00030-03, Adipo bioscience, USA) Angiotensin 1-7 (Ang 1-7, E02A0225, BlueGene Biotech, China), Il6 (R6000B, R&D Systems, UK) and TNFα (ER3TNFA, Thermo Scientifics, USA) were measured according to the manufacturer's instructions. Results were analyzed using an ELISA plate reader (UVM-340, ASYS Hitech GmbH, Austria) and a calibration curve was constructed by plotting the absorbance values at 450nm (with specific correction, according to manufacturer's protocol) and concentrations of unknown samples were determined.

## 4. Array protein expression profile

The expression of some inflammation related-proteins was performed using plasma samples and a Rat Adipokine Array Kit (ARY016, R&D systems, UK).

Nitrocellulose membranes were blocked for 1 hour with an array buffer and then a cocktail of biotinylated detection antibodies was added and incubated overnight at 4ºC. The membranes were washed several times in order to remove all the unbound material. Streptavidin-HRP, an enzyme used for the detection of the substrate was applied, incubated for 30 minutes and washed. Finally Chemi Reagent Mix was added and the signal produced was measured in a chemiluminescence detection system (ChemiDoc™ MP, Bio-Rad, USA).

## 5. Histology, cardiomyocyte and aorta dimensions

LV and descending aortic samples were fixed in 4% paraformaldehyde, dehydrated with gradual ethanol, cleared with xylene and were included in paraffin blocks. Serial sections with 4 µm of thickness were cut using a microtome (RM2125RTS, Leica, Germany) and mounted on slides. Next the slides were dewaxed in xylene, hydrated through a series of decreasing concentration of alcohol solutions and stained for haematoxylin-eosin. Slides were subsequently submitted to a new series of decreasing concentration of alcohol solutions and xylene and finally mounted with Entellan (Merck, Germany).

Cardiomyocyte cross-sectional area, descending aortic diameter and thickness were determined observing slides at light microscopy (Dialux 20, Leitz, Germany) and using image acquisition software (cell B, Olympus, USA).

## 6. AGEs immunohistochemistry

Immunohistochemistry was performed to determine AGEs expression in myocardium and in 25-50, 50-100, and >100 vessels caliber. Four- µm LV apex sections were sliced, placed and subjected to deparaffinization and rehydration.

A heat solution of sodium citrate buffer 10mM ($C_6H_5Na_3O_7.2H_2O$, pH 6.0) was added for 30 minutes into the slides to induce antigen retrieval. All sections were encircled with a hydrophobic pen (Immunopen, Immunologic, Netherlands) to prevent splitting leakage and the endogenous peroxidase activity was blocked using 100µL/section of a 3% hydrogen peroxide solution (Sigma Aldrich, USA) and incubated at room temperature for 10 minutes. All slides were washed with distillated $H_2O$ ($dH_2O$) and with Tris-Buffered Saline-Tween (TBST; 100 mM Tris, 1.5 mM NaCl, pH 8.0 and 0.1% Tween-20) for 5 minutes with agitation. Blockage of non-specific binding was prepared with 5% normal goat serum (NGS, ab7481, abcam, Cambridge, UK) in TBST,

added 100 µL for section and incubated at 1 hour at room temperature. Next all slides were washed 3 times for 5 minutes with TBST with agitation. Blockage of endogenous avidin-biotin expression was preform at room temperature using an endogenous avidin + biotin blocking system (ab3387, abcam, Cambridge, UK) according to manufacturer's instructions (1 drop and 15 minutes of incubation). The primary antibody (Anti-AGE primary antibody, ab23722, abcam, UK) in a 1/500 dilution was incubated at 4ºC overnight. After incubation slides were washed 3 times for 5 minutes with TBST and with agitation and were incubated with the secondary antibody (goat anti-rabbit IgG, ab6720, abcam, UK) in a 1/250 dilution at room temperature for 2 hours. Slides were next washed with agitation 3 times for 5 minutes with TBST. All slides were incubated with 3.3-diaminobenzidine (DAB, ab94665, abcam, UK) at room temperature until brown color was observed. Then slides were washed with $dH_2O$ and counterstained with Gill haematoxylin (Merck, Germany) for 3 minutes. Finally all slides were submitted to decreasing concentration of alcohol solutions, xylene and mounted with Entellan (Merck, Germany).

Negative control was made with the omission of the primary antibody. The slides were observed and photographed with a microscope (Dialux 20, Leitz, Germany) and AGE's quantification was made using Image Pro Plus 6 software (MediaCybernetics, USA).

## 7. Western Blotting

LV samples were homogenized on ice in 1 ml RIPA lysis buffer (150 mM NaCl, 1.0% IGEPAL® CA-630, 0.5% sodium deoxycholate, 0.1% SDS, and 50 mM Tris, pH 8.0) containing the following protease inhibitors: phenylmethylsulfonyl fluoride (1mM), aprotonin ($10 g.ml^{-1}$), leupeptin ($10 \mu g.ml^{-1}$) and pepstatin ($10 \mu g.ml^{-1}$), all from Sigma Chemicals (USA). Samples were then centrifuged at 11000 rpm for 20 minutes at 4°C. The supernatants were collected and total protein concentration was determined.

Samples containing 20 µg of protein were loaded on a 6% SDS Polyacrylamide gel (SDS-PAGE), run and electroblotted into polyvinylidene difluoride membrane. Pre-stained molecular weight marker proteins were used as standards for the SDS-PAGE. Ponceau staining was performed to verify the quality of the transfer and to ensure equal protein loading. Blots were blocked in 5% non-fat skimmed milk in PBS for 1 hour, treated overnight with antibody against the different proteins (eNOS, 9572, Cell Signaling Technology, USA; β-actin, 4967, Cell Signaling Technology, USA; p-eNOS, 9571, Cell Signaling Technology, USA) followed by incubation with alkaline phosphatase secondary antibodies for 1 hour. Immunoblots were developed with an ECF$^{TM}$ Western blotting detection system (GE Healthcare, UK). Protein content was determined using a Bio-Rad protein assay kit.

## 8. Cardiac endothelial cells isolation

A LV sample was cut and transferred into a gentleMACS C tube (Miltenyl Biotec, Germany) containing HBSS ($CaCl_2$, $MgCl_2$, Lifetechnologies,USA) with collagenase II (Worthington, USA) and DNase I (Applichem, USA). The C tube was connected to the gentleMACS dissociator (Miltenyl Biotec, Germany) and the sample was incubated for 30 minutes at 37ºC with agitation every 5 minutes in order to resuspend the settled tissue fragments. Next the C tube was runned out again in the gentleMACS dissociator. In the end, the solution was passed into a 70µm cell strainer (Corning, USA), washed with cold HBSS and the cell suspension suffered a spin down at 1500 rpm for 10 minutes at 4ºC. Cold HBSS was immediately added and the cell suspension suffered a new spin down at 1500 rpm for 10 minutes at 4ºC. Next cells were washed with FACS medium (eBioscience, USA), suffered another spin down at 1500 rpm for 10 minutes at 4ºC and resuspended in HBSS (1ml/heart).

## 9. Flow cytometry and sorting

Cardiac endothelial cells were resuspended in ice-cold FACS medium (eBioscience, USA) and added into a 96 well plate (105-106 cells/well) in a way that surrounding each well stays an empty one. FACS medium was added, the plate was washed by centrifugation for 5 minutes for 2000 rpm and supernatant was discarded. CD90 Pacific blue (Biolegend, USA), PE anti-rat CD54 (Biolegend, USA), CD44 Purified (BD Biosciences, USA) and CD106-Pe (BD Biosciences, USA) antibodies were added in a dilution in FACS medium to a maximum volume of 25-50 µl and incubated on ice for 20 minutes protected from light. FACS medium was added and the plate was washed by centrifugation for 5 minutes for 2000 rpm. The supernatant was discarded. In order to loose cells, the plate suffered a shacking in a vortex set at medium speed. Cells were transferred into FACS tubes (eBioscience, USA) with the remaining volume up to a total of 400µL. The tubes were protected from light and read it in FACS (eBioscience, USA) and cells suffer cell sorting.

## 10. RNA extraction and reverse transcription

LV sample from each animal was cut and putted in tubes with 500 µl Tripure each (Roche, USA). In a fume hood each tube was homogenized and then incubated in room temperature for 5 minutes. Chloroform was added on all tubes, which suffered a rapid vortex, and then were incubated for 10 minutes in room temperature. Next all tubes were centrifuged at 15000 rpm at 4ºC for 15 minutes and the resulting aqueous phase was collected to a new tube with isopropanol. The tubes suffered a rapid vortex and were incubated at room temperature for 10 minutes. In the end all were centrifuged at 15000 rpm at 4ºC for 10 minutes and the supernatant was discarded. The resulting pellet was washed with 70% ethanol and a rapid vortex was made. The tubes were centrifuged for 5 minutes at 15000 rpm at 4ºC, the supernatant was discarded again and the tubes were left opened and turned down in order to completely dry the pellet. RNase free water (Qiagen, Netherlands) was added

and for 30 minutes all tubes were left on ice to dissolve the pellet. In the end all tubes suffered a vortex and reverse transcription protocol.

RNA concentration from all samples was adjusted in order to perform a 1µg of total RNA in a 20 µL volume. Random Primers in a 1/5 concentration were added to the samples and were incubated for 20 minutes at room temperature and 3 minutes on ice.

A mix containing 5X buffer (Invitrogen, USA), dNTPs (Invitrogen, USA), DTT (Invitrogen, USA), RNase free water (Qiagen, Netherlands), RNasin (Promega, USA), $MgCl_2$ (Thermo Scientific, USA) and SuperScript II (Invitrogen, USA), was made and distributed to each sample. Two negative controls were also prepared: no template control (NTC) in which samples were substituted by RNase free water to verify if reagents were contaminated; and $RT^-$ in which SuperScript II is substituted by RNase free water to verify if samples are contaminated with genomic DNA. The reaction mixtures were incubated in Thermocycler (Biometra, Germany) in 25ºC for 10 minutes, 42ºC for 50 minutes and 70ºC for 15 minutes.

## 11. Real time - PCR

Real-time PCR was performed StepOnePlus™ Real-Time PCR System (Applied Biosystems, USA) with myocardium cells, using 96-well 0.1 ml PCR plates (Applied Biosystems, USA) and carried out with SYBR Green 2X Master Mix (Qiagen, Netherlands). The primers were obtained from Thermo Scientific (Germany). Amplification reactions were performed in duplicate and the amount of RNA in the reactions was normalized with an internal control, the constitutively expressed gene Glyceraldehyde 3-phosphate dehydrogenase (GAPDH) as its mRNA levels were similar between groups. Gene expression was quantified using the comparative Ct method ($2^{-\Delta Ct}$), where $\Delta Ct = Ct_{target\ gene} - Ct_{GAPDH}$.

## 12. Vascular function

Aortic rings with about 1.5 mm were isolated from ascending aorta samples and assembled between metal pins in an organ bath system (770MO, Danish Myo Technology). After stabilization, a curve of passive tension-length by progressive mono-axial stretching was obtained of the vascular rings at intervals of 20%, since the diameter with no tension - without stretching ($L_0$) until 200% of $L_0$. The strain (Ɛ) was defined as the proportional increase of length in relation to $L_0$. The passive tension curve was mathematically modulated by an exponential function, in which β is a vascular stiffness index. In every step an active tension curve with KCl stimulation was obtained. After passive tension adjustment of the vascular ring, and considering a resting transmural pressure of 100 mmHg, vascular reactivity was evaluated thought an dose-response curve to phenylephrine (Phe; $10^{-9}$ to $10^{-5}$, in logarithmic 0.5 intervals) and the endothelial function thought an dose-response curve to acetylcholine (Ach; $10^{-9}$ to $10^{-4}$, in logarithmic 0.5 intervals), being the relaxation evaluated according to the percentage of decrease, after pre-contraction with Phe. Acquisitions were made using LabChart 7 Pro v7.3.1 (ADInstruments, New Zealand).

## 13. Statistical analysis

Statistical analysis was performed using Graph Pad Prism software (version 5.0, Graph Pad software, USA). One-way ANOVA test was used for comparison among groups and two-way repeated-measures ANOVA test was used to performed analysis for repeated measures for the same animal. Single comparisons were assessed by an unpaired Student t test. Group data are presented as means ± SEM. Results were considered significantly different when $p<0.05$.

# Part 4

## Results

*“Science, in the very act of solving problems, creates more of them.”*

Abraham Flexner

# 1. Characterization of the animal model

## 1.1. Morphometric data

Morphometric parameters were normalized to TL and are presented in Table 3. Body weight is significantly higher in ZSF1Ob when comparing ZSF1Ln and WKY and both ZSF1 groups are heavier than WKY. Regarding cardiac hypertrophy, ZSF1Ob and ZSF1Ln present increased LV weight/TL (Table 3), further confirmed histologically by their larger cardiomyocytes diameter (Figure 5) and echocardiographically by an augmented LV mass (Table 4). ZSF1Ob presented several organs that were significantly heavier than ZSF1Ln and WKY, such as perigonadal and perirenal fat, as expected in an obese model, and lung/TL, consistently with lung congestion. Gastrocnemius muscle weight normalized to TL was lower in ZSF1Ob when compared to ZSF1Ln, revealing cachexia (Table 3).

**Table 3.** Morphological data from WKY (n=17), ZSF1Ln (n=14) and ZSF1Ob (n=18) animals. LV, left ventricle; RV, right ventricle; TL, tibial length. The values are represented as means ± S.E.M. p<0.05: * vs WKY, † vs ZSF1Ln.

| Morphometric parameters | WKY | ZSF1Ln | ZSF1Ob |
|---|---|---|---|
| Weight (g) | 358.93±5.9 | 434.32±8.5* | 606.13±6.6*† |
| TL (mm) | 39.75±0,8 | 43.10±1,0* | 40.68±0.4† |
| Heart weight/TL ($mg.mm^{-1}$) | 32.52±1.1 | 34.08±1.1 | 40.25±0.9*† |
| RV weight/TL ($mg.mm^{-1}$) | 3.08±0.3 | 2.38±0.3 | 4.57±0.5† |
| LV weight/TL ($mg.mm^{-1}$) | 8.56±0.8 | 9.44±0.8 | 10.81±0.5* |
| Lung weight/TL ($mg.mm^{-1}$) | 41.59±2.2 | 44.08±2.3 | 63.73±4.0*† |
| Spleen weight/TL ($mg.mm^{-1}$) | 15.18±1.0 | 16.69±1.0 | 21.58±1.1*† |
| Pancreas weight/TL ($mg.mm^{-1}$) | 12.41±1.6 | 13.68±1.8 | 21.85±5.9 |
| Liver weight/TL ($mg.mm^{-1}$) | 275.32±9.1 | 324.15±11.8 | 936.36 ± 37.2*† |
| Kidney weight/TL ($mg.mm^{-1}$) | 60.30±1.6 | 71.48±2.1 | 106.68±2.6*† |
| Perirenal fat weight/TL ($mg.mm^{-1}$) | 62.32±4.3 | 52.64±5.7 | 372.30±10.3*† |
| Perigonadal fat weight/TL ($mg.mm^{-1}$) | 57.82±3.1 | 58.28±3.5 | 137.19±6.4*† |
| Gastrocnemius weight/TL ($mg.mm^{-1}$) | 54.31±1.0 | 62.17±1.7* | 51.06±1.1† |

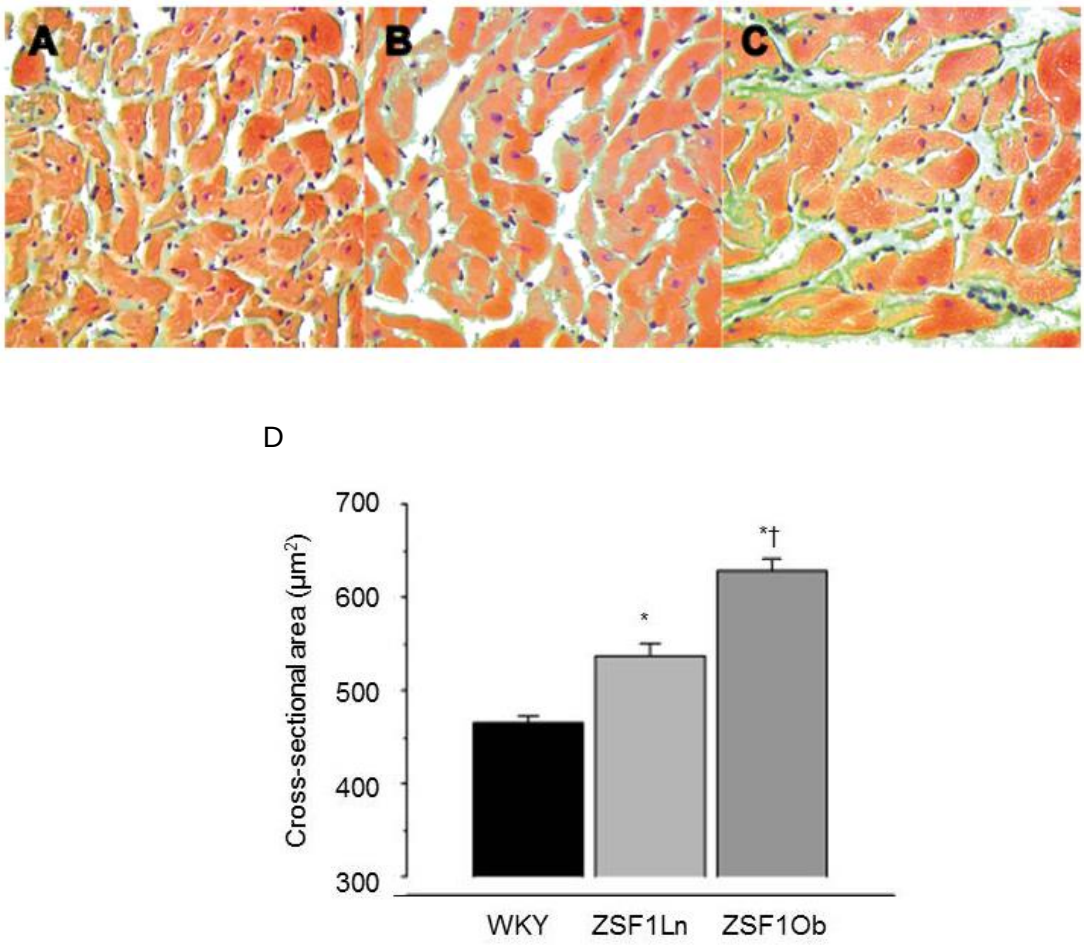


**Figure 5.** Cardiomyocyte hypertrophy represented by its cross-sectional area (D). Representative images of hematoxylin-eosin stained section of LV from WKY (n=5, A), ZSF1Ln (n=5, B) and ZSF1Ob (n=5, C). The values are represented as means ± S.E.M. $p<0.05$: * vs WKY, † vs ZSF1Ln.

### 1.2. Cardiac functional and structural changes

Echocardiographic evaluation showed that ZSF1 groups presented preserved systolic function, as observed by similar cardiac index (CI), ejection fraction (EF) and end-diastolic volume index (EDVI) values. Global cardiac performance, assessed by the Tei index was similar between groups (Table 4).

In contrast with systolic parameters, significant disturbances in diastolic function were observed in ZSF1Ob animals compared to ZSF1Ln and WKY groups, namely, an increase in the maximum velocity of early diastolic

transmitral flow to maximum velocity of myocardial displacement ratio at the lateral mitral annulus also in early diastole (E/E') and a decrease in early and late LV filling velocities ratio (E/A). In addition, an increased left atrium area (LAA) was observed in ZSF1Ob (Table 4).

**Table 4.** Echocardiographic evaluation of WKY (n=7), ZSF1Ln (n=9) and ZSF1Ob (n=15) animals at 18$^{th}$ week. CI, cardiac index; EF, ejection fraction; MPI, myocardial performance index – Tei index; FS, fractional shortening; CO, cardiac output; LV, left ventricle; S', mitral annular systolic velocity; SV, stroke volume; BSA, body surface area; ESVI, end-systolic volume index; ESDVI, end-diastolic volume index; E/E', ratio of mitral velocity to early diastolic velocity of the mitral annulus; E/A, early and late LV filling velocities ratio; LAA, left atrium area; HR, Heart rate. The values are represented as means ± S.E.M. p<0.05: * vs WKY, † vs ZSF1Ln.

| **Echocardiographic parameters** | **WKY** | **ZSF1Ln** | **ZSF1Ob** |
|---|---|---|---|
| CI ($mL.min^{-1}.cm^{-2}$) | 215.28 ± 21.20 | 193.49 ± 15.53 | 242.50 ± 12.89 |
| EF (%) | 72.82 ± 3.28 | 74.30 ± 2.46 | 75.72 ± 1.19 |
| MPI (Tei index) | 0.77 ± 0.04 | 0.74 ± 0.06 | 0.71 ± 0.03 |
| FS (%) | 37.39 ± 2.66 | 38.61 ± 2.00 | 40.00 ± 1.03 |
| CO ($L.min^{-1}$) | 95.10 ± 10.45 | 95.36 ± 7.43 | 152.87 ± 8.70*† |
| LVmass MM (mg) | 0.57 ± 0.08 | 0.76 ± 0.10 | 0.92 ± 0.06* |
| S' ($mm.s^{-1}$) | 0.03 ± 0.003 | 0.05 ± 0.01 | 0.05 ± 0.004 |
| SV (mL) | 0.33 ± 0.04 | 0.29 ± 0.02 | 0.49 ± 0.03*† |
| BSA ($cm^2$) | 439.83 ± 8.21 | 493.27 ± 6.27 | 628.19 ± 3.94*† |
| ESV I ($mL/cm^{-2}$) | 0.47 ± 0.06 | 0.50 ± 0.07 | 0.50 ± 0.04 |
| EDV I ($mL/cm^{-2}$) | 1.75 ± 0.11 | 1.89 ± 0.11 | 2.10 ± 1.11 |
| E/E' | 12.62 ± 0.62 | 12.06 ± 0.45 | 16.34 ± 0.43*† |
| E/A | 1.80 ± 0.11 | 1.57 ± 0.10 | 1.22 ± 0.05*† |
| LAA ($mm^2$) | 0.21 ± 0.02 | 0.25 ± 0.01 | 0.36 ± 0.01*† |
| HR (bpm) | 290.53 ± 14.25 | 329.33 ± 11.16 | 318.91 ± 10.37 |

## 2. Aorta characteristics and vascular function

Regarding structural changes, abdominal aorta from WKY and from both ZSF1 groups was analyzed and the diameter and thickness measured. Aortas from ZSF1Ob animals were clearly bigger (Figure 6A) and the diameter was significantly higher in both ZSF1 groups (Figure 6B). Regarding aortic thickness, ZSF1Ob aortas showed a tendency to be thicker relatively to the other two groups (Figure 6C). Interestingly, AGEs deposition was higher in vessels from WKY, meaning that AGEs were not responsible for vessels stiffening (Figure 6 D, E & F).


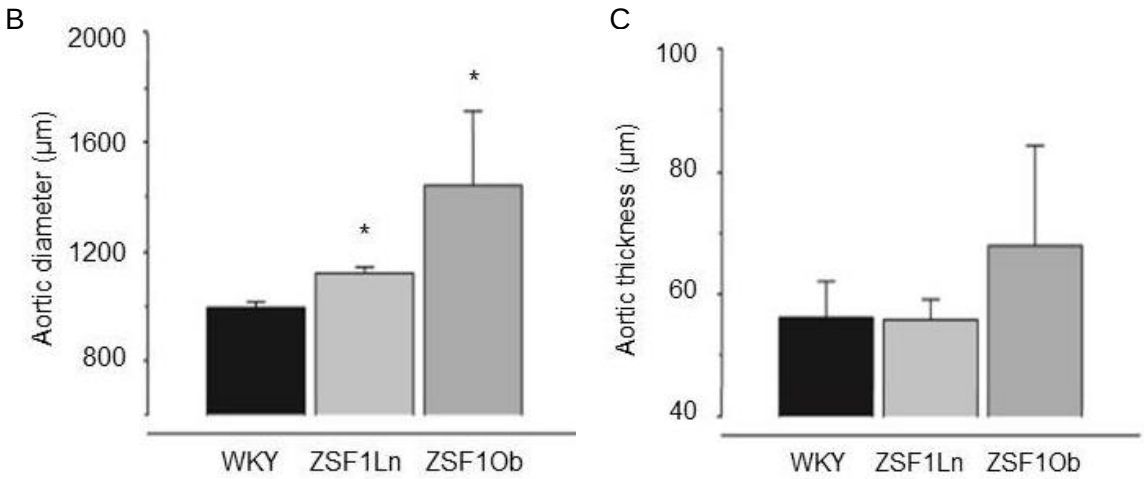

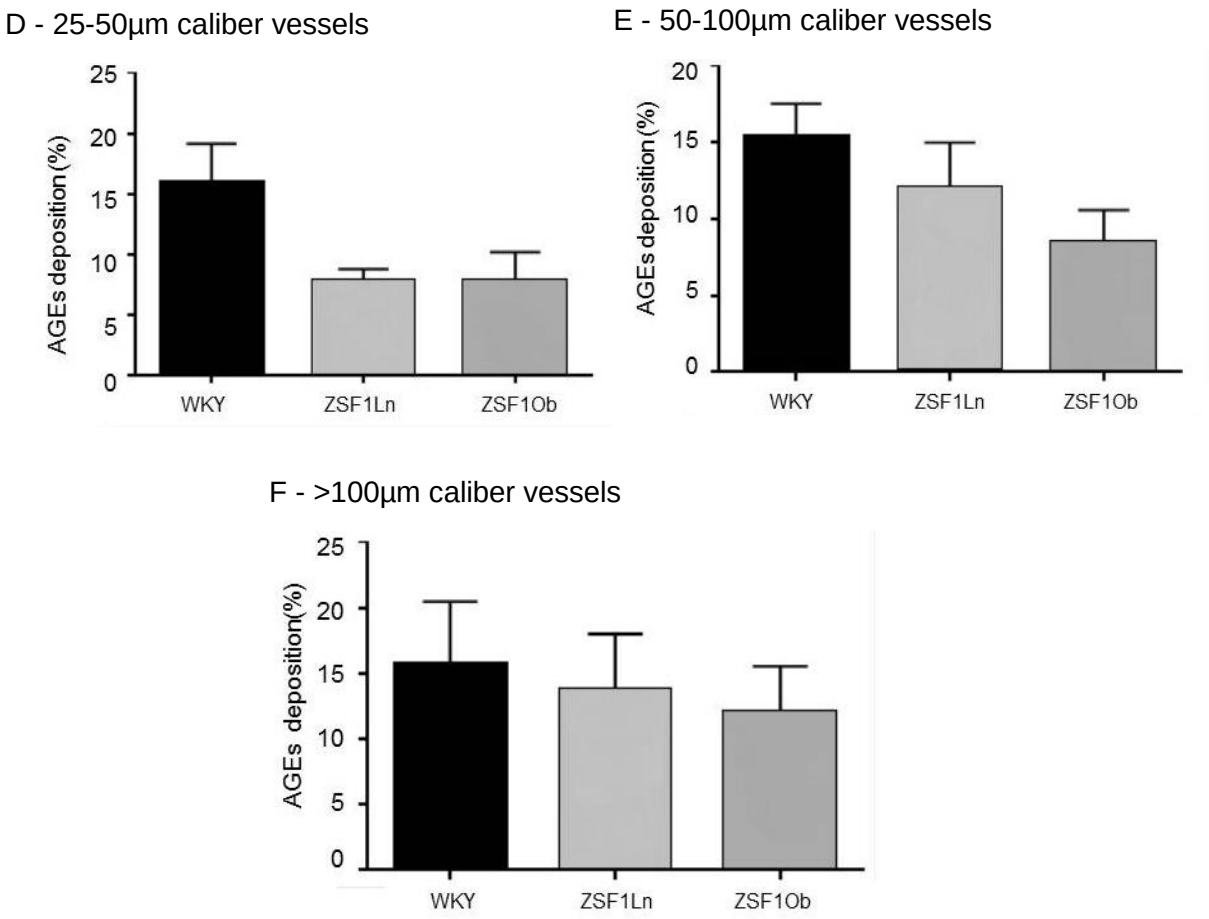


**Figure 6.** Descending aorta characteristics of WKY (n=5), ZSF1Ln (n=5) and ZSF1Ob (n=5) animals. A) Representative images of aorta morphology; B) Aortic diameter and C) Aortic thickness; D) 25-50µm caliber vessels AGEs; E) 50-100µm caliber vessels AGEs; F) >100µm caliber vessels AGEs. The values are represented as means ± S.E.M. $p<0.05$: * vs WKY.

In terms of function, after stretching the aortic rings, the passive tension (Figure 7A) and the strain stiffness index was higher in ZSF1Ob (1.45±0.28, $p<0.05$) than in ZSF1Ln and WKY (1.12±0.06 and 0.89±0.04, $p<0.05$, respectively).

Aortic rings were exposed to increasing concentrations of Phe to evaluate the vascular reactivity and the developed maximum active tension was significantly higher in ZSF1Ob group compared to WKY and ZSF1Ln groups (Figure 7B). ZSF1Ob group also displayed impaired relaxation (42±2%, $p<0.05$) comparing to ZSF1Ln and WKY (56±6% and 84±3%,

p<0.05, respectively) after the incubation with increasing concentrations of Ach (Figure 7C).

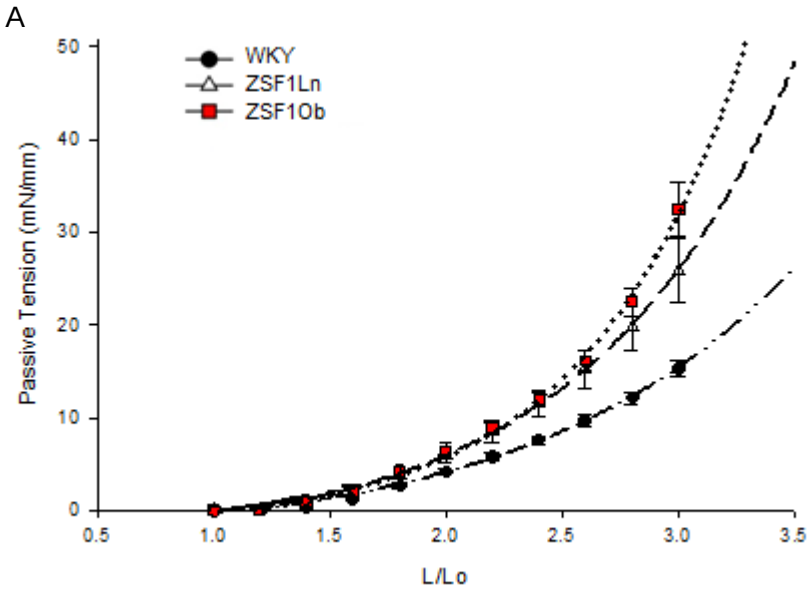


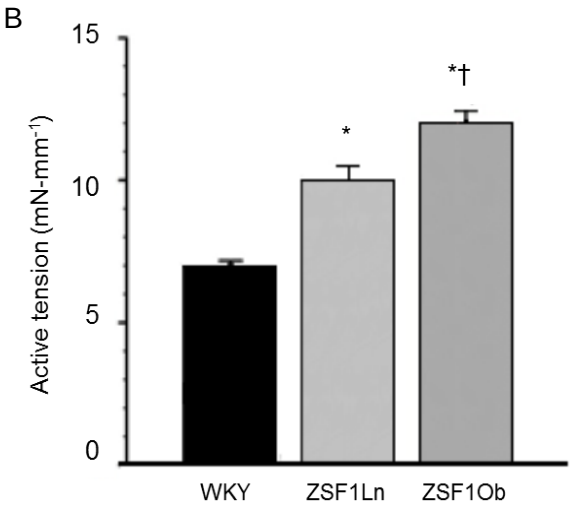

C

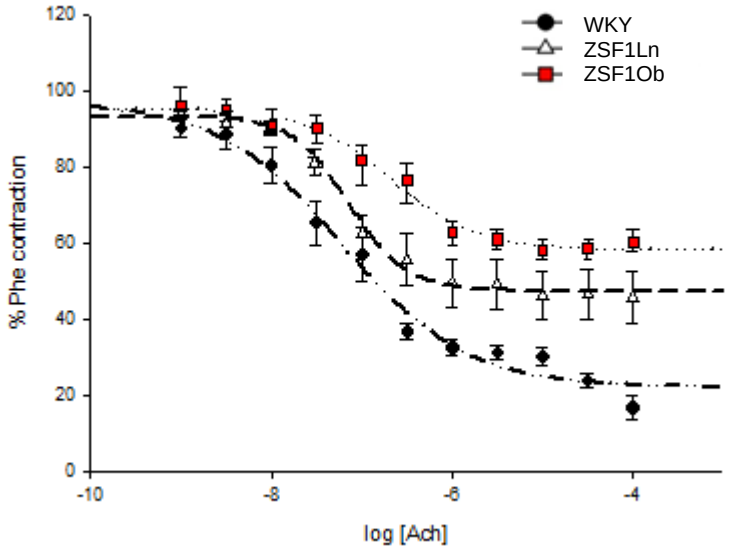


**Figure 7.** Vascular function of aortic rings from WKY (n=5), ZSF1Ln (n=5) and ZSF1Ob (n=5), animals. A) Strain-passive tension curve; B) Maximum active tension at phenylephrine (Phe) maximal concentration ($10^{-5}$); C) Vascular relaxation to increasing doses of acetylcholine (Ach) pre-contracted with Phe. The values are means ± S.E.M. $p<0.05$: * vs WKY, † vs ZSF1Ln.

## 3. Plasma levels of adipokines and inflammatory markers

We performed a rat adipokine array kit to have an overview of the major plasma changes in ZSF1Ob versus ZSF1Ln using a small number of samples per group. Results are presented in table 5 and revealed that the expression of pro-inflammatory cytokines Il-1β and Il-6 displayed a small tendency to be lower in ZSF1Ob group when compared to ZSF1Ln. In contrast, the expression of ICAM1 showed a trend to increase in ZSF1Ob. No differences were found in relation to anti-inflammatory cytokines Il-11 and Il-10 (Table 5). Interestingly, only levels of monocyte chemoattractant protein 1 (MCP1), that actively recruits leukocytes into inflammatory sites, were significantly higher in ZSF1Ob. Lipocalin, a protein involved in the lipid transport which also has a role in inflammation, displayed a trend to have higher levels in the obese rats (Table 5).

**Table 5.** Plasma protein expression (% of change from the positive control) assessed by a profile array of ZSF1Ln (n=4) and ZSF1Ob (n=4) animals. Il-1β, interleukin-1β; Il-6, interleukin-6; TNFα, tumor necrosis factor α; ICAM1, intercellular adhesion molecule 1; Il-11, interleukin-11; Il-10, interleukin-10; MCP1, monocyte chemoattractant protein 1; RANTES, regulated on activation, normal T cell expressed and secreted. The values are represented as means ± S.E.M. $p<0.05$: † vs ZSF1Ln.

| Protein (%) | ZSF1Ln | ZSF1Ob |
|---|---|---|
| Il-1β | 6,1 | 4,0 |
| Il-6 | 2,9 | 1,8 |
| TNFα | 2,5 | 2,8 |
| ICAM1 | 16,3 | 21,3 |
| Il-11 | 3,8 | 3,7 |
| Il-10 | 2,6 | 2,2 |
| MCP1 | 19,2 | 54,3 † |
| RANTES | 7,5 | 4,5 |
| Lipocalin | 45,1 | 58,2 |

We further confirmed some circulatory parameters by ELISA (Table 6), a more sensitive technique that revealed that plasma levels of leptin were significantly increased and there was a similar trend in FABP4 levels, consistently with metabolic syndrome (Table 6). In both ZSF1 groups, the vasodilator Ang 1-7 was significantly increase ($p<0.05$) to compensate for the increased ventricular overload and arterial stiffness present in these hypertensive groups (Table 6).

Interestingly, plasma levels of pro-inflammatory cytokines such as Il-6 and TNFα revealed a tendency to be higher in WKY group while, between ZSF1 groups, obese animals displayed slightly lower values than the lean ones, consistently with the array results (Table 6).

**Table 6.** Circulating plasma levels data from WKY (n=6), ZSF1Ln (n=9) and ZSF1Ob (n=8) groups. FABP4, fatty acid binding protein 4; Ang 1-7, angiotensin 1-7; Il-6, Interleukin-6; TNFα, tumor necrosis factor α. The values are represented as means ± S.E.M. p<0.05: * vs WKY, † vs ZSF1Ln.

| Protein | WKY | ZSF1Ln | ZSF1Ob |
|---|---|---|---|
| Leptin ($pg.mL^{-1}$) | 434.34 ± 136.67 | 405.77 ± 240.23 | 22150.15±10711.55*† |
| FABP4 ($ng.mL^{-1}$) | 53.03 ± 18.53 | 83.27 ± 64.86 | 122.18 ± 81.34 |
| Angiotensin 1-7 ($ng.mL^{-1}$) | 1.84 ± 0.85 | 3.16 ± 1.04* | 3.28 ± 0.46* |
| Il-6 ($pg.mL^{-1}$) | 277.38 ± 218.29 | 176.67 ± 146.84 | 134.45 ± 68.92 |
| TNFα ($pg.mL^{-1}$) | 76.44 ± 42.15 | 71.57 ± 43.85 | 55.38 ± 15.44 |

## 4. Markers of myocardial dysfunction

In addition, myocardial expression of some inflammatory-related and ROS-related genes and proteins was also measured by real-time PCR and western blotting and are shown in figures 8&9.

When it comes to gene expression of endothelial function-related genes, E-selectin expression was higher in ZSF1 group (p<0.05), while in ICAM1, VCAM1, eNOS3 and endothelin 1 no significant differences were observed but only a trend towards their upregulation (Figure 8).

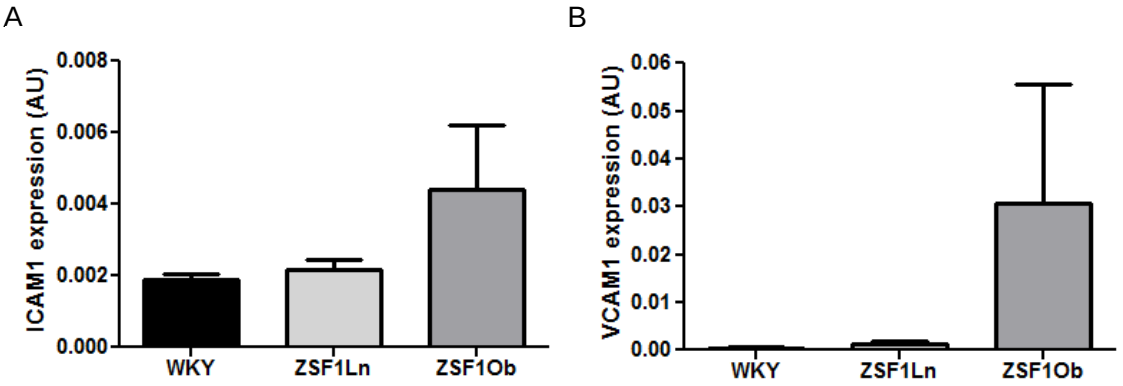

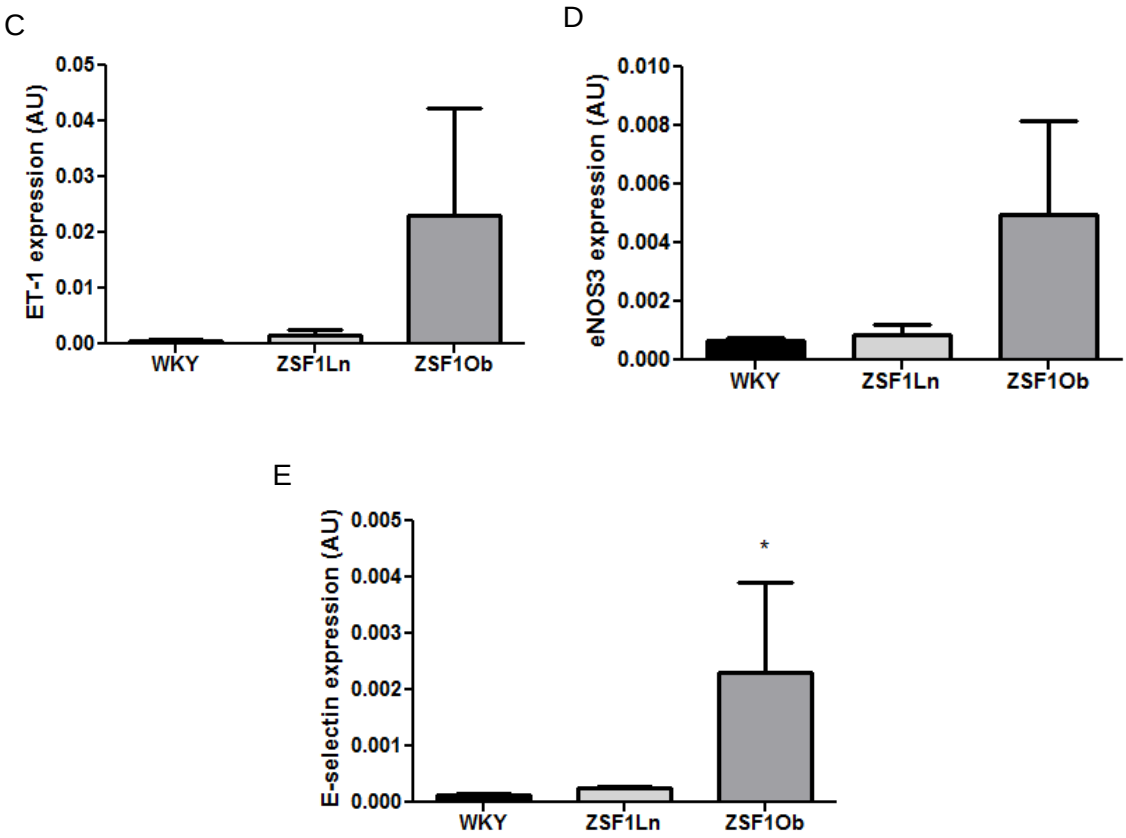


**Figure 8.** mRNA expression of WKY (n=5), ZSF1Ln (n=5) and ZSF1Ob (n=5) animals. A) ICAM1, intercellular adhesion molecule 1; B) VCAM1, vascular cell adhesion molecule 1; C) endothelin 1; D) eNOS, endothelial nitric oxide synthase; E) E-selectin. The values are represented as means ± S.E.M. $p<0.05$: * vs WKY.

The expression of AGEs receptor (RAGEs) was not different between the ZSF1 groups (Figure 9A), but both results were significantly higher than WKY. AGES deposition, assessed by carboxymethyllysine (CML) expression, was similar between groups despite a trend towards an increase in ZSF1Ob (Figure 9B). Vasodilator-stimulated phosphoprotein (VASP) (Figure 9C) and eNOS protein (Figure 9D) expression had no differences.

In ZSF1Ob rats, NOX2 expression, which promotes ROS production, increased in a significant way, compared with WKY and ZSF1Ln. Contrarily, NOX4 expression in ZSF1Ob, with protective properties against ROS, was significantly lower than the other groups (Figure 9E&F).

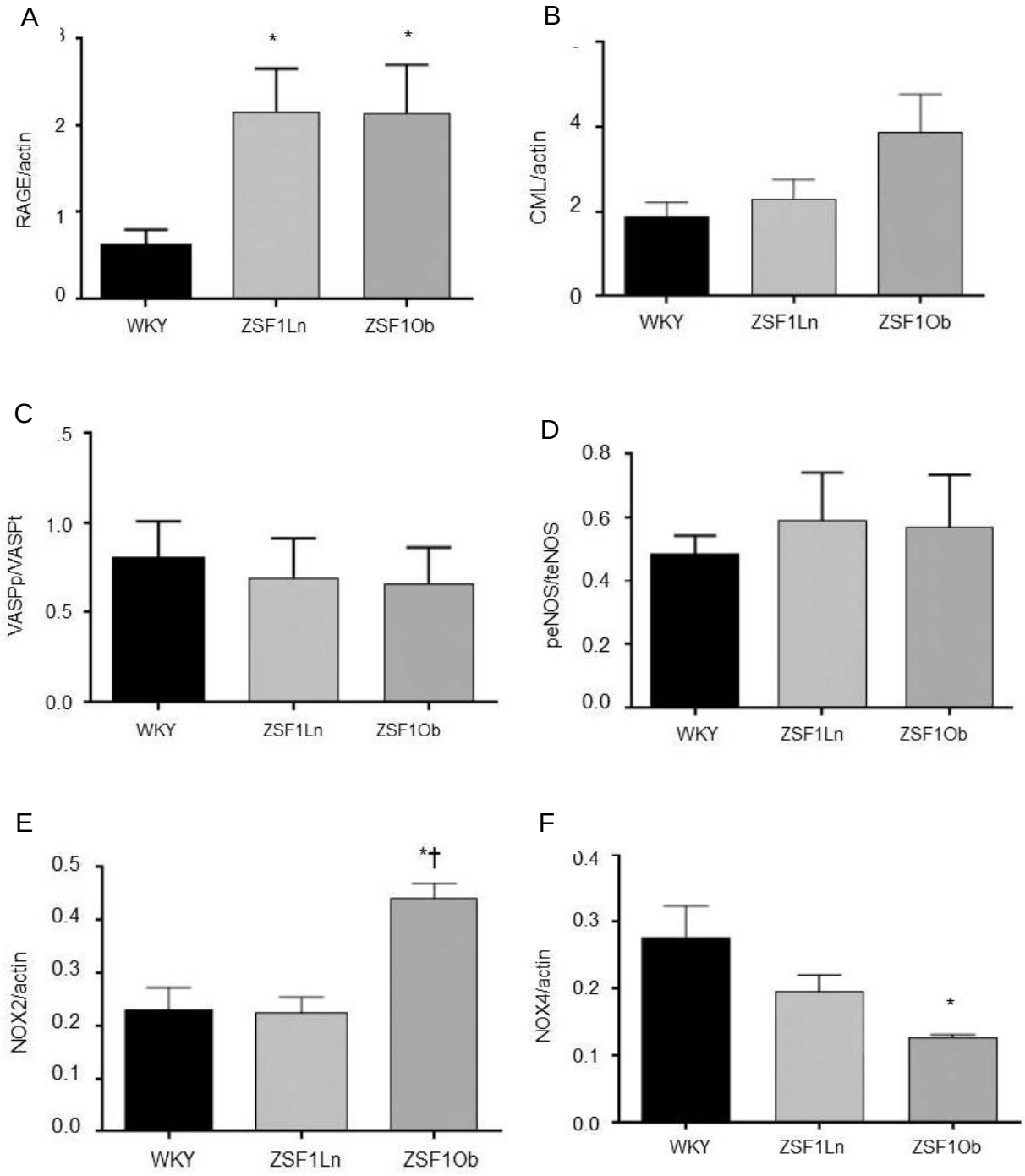


**Figure 9.** Protein expression of WKY (n=6), ZSF1Ln (n=6) and ZSF1Ob (n=5) animals assessed by western blotting. A) RAGE, receptor of AGEs; B) CML, carboxymethyllysine; C) VASP, vasodilator-stimulated phosphoprotein; D) eNOS, endothelial nitric oxide synthase; E) NOX 2, NADPH oxidase 2; F) NOX 4, NADPH oxidase 4. The values are represented as means ± S.E.M. $p<0.05$: * vs WKY, † vs ZSF1Ln.

## 5. Flow cytometry analysis

Representative scatter plots of flow cytometry analysis is depicted in figures 10A&B. Flow cytometry analysis revealed similar levels of CD31, a marker of endothelial cells, between ZSF1Ln and ZSF1Ob groups (Figure 10C). Differently, ZSF1Ob LV samples display a significantly higher number of CD45 positive cells (Figure 10D), a marker of inflammation.

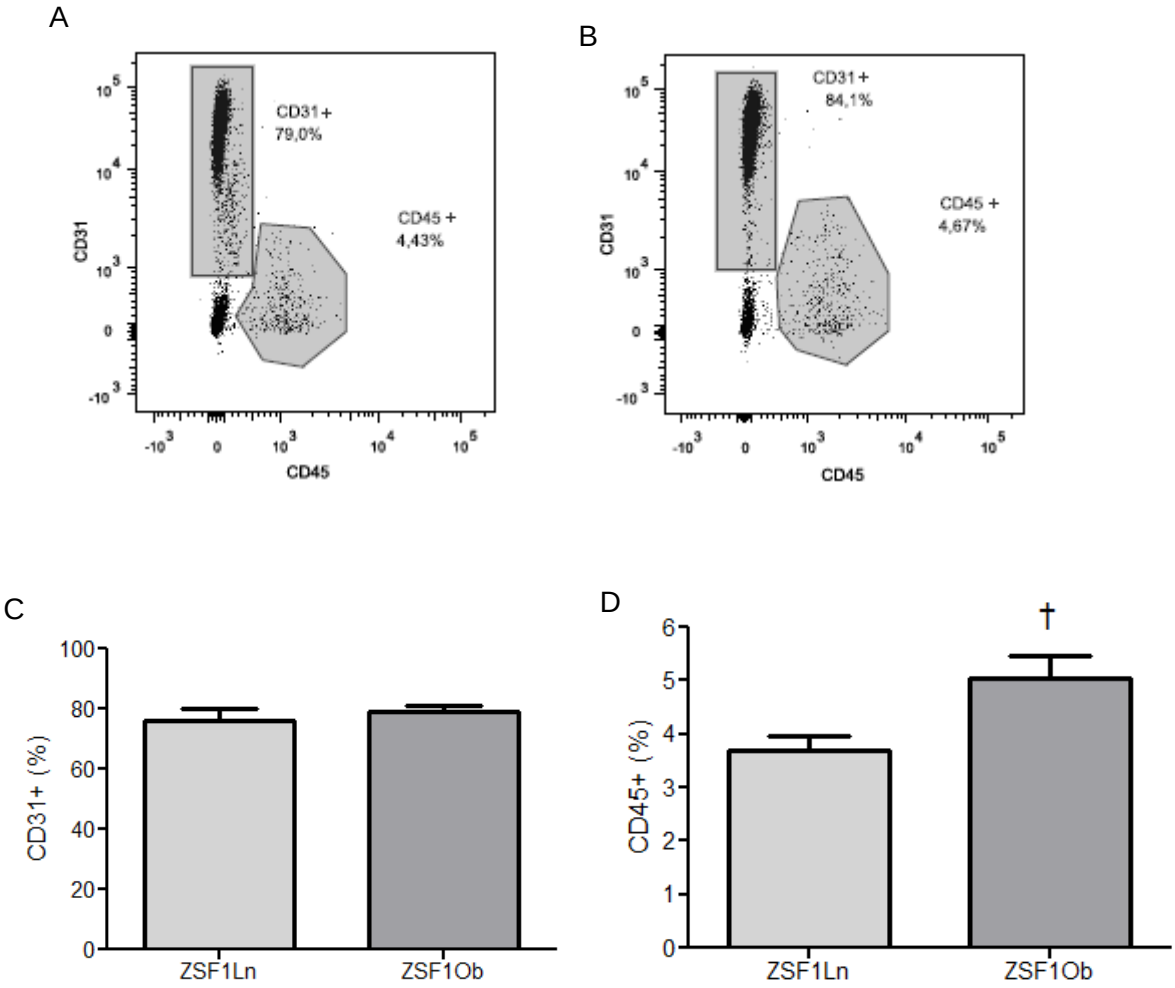


**Figure 10.** Flow cytometry analysis. (A) Example of a representative plot of CD31 versus CD45 expression from a ZSF1Ln animal. (B) Example of a representative plot of CD31 versus CD45 expression from a ZSF1Ob animal. (C) Expression of CD31+ cells in ZSF1Ln (n=3) and ZSF1Ob (n=5). (D) Expression of CD45+ cells in in ZSF1Ln (n=3) and ZSF1Ob (n=5). The values are represented as means ± S.E.M. $p<0.05$: † vs ZSF1Ln.

# Part 5

## Discussion

*“The important thing in science is not so much to obtain new facts as to discover new ways of thinking about them.”*

William Lawrence Bragg

The present study explored a previously described animal model of HFpEF, the ZSF1 obese rat, aiming to identify the pathophysiologic mechanisms underlying diastolic dysfunction progression. We have shown that the highly prevalent comorbidities associated to HFpEF trigger inflammation, oxidative stress and endothelial dysfunction in this animal model.

## 1. Metabolic risk-related HFpEF model

In this study we used the ZSF1 animal model and demonstrated that ZSF1Ob develops HFpEF at their 20$^{th}$ week of age. Compared to ZSF1Ln or WKY rats, ZSF1Ob showed many features of high metabolic risk such as visceral obesity evident from elevated perirenal and perigonadal fat, insulin resistance, hyperglycemia and physical inactivity evident from striated muscle wasting. ZSF1Ob rats present two different mutations for leptin receptor gene and as a compensatory response, leptin levels significantly increase. Lipocalin and FABP4 levels are also elevated in ZSF1Ob group, showing that in these rats adipose tissue is already dysfunctional and secreting a different pattern of adipokines.

Comparing with WKY group, ZSF1Ln presented hypertension and consequent LV hypertrophy both at the organ and cellular level, which was further aggravated in ZSF1Ob rats. This hypertrophic response represents an attempt to normalize increased ventricular wall stress imposed by systemic arterial hypertension. Indeed, hypertrophy parallels the cardiac remodeling associated to HFpEF, namely in terms of ventricular size, geometry, shape and composition. Besides obesity, ZSF1Ob animals also developed hyperglycemia, oral glucose intolerance, insulin resistance, glycosuria and DM, all features that trigger diastolic dysfunction progression towards HFpEF [57]. Indeed, this represents an interesting aspect of ZSF1 as we were able to demonstrate that overload imposed by hypertension, as in ZSF1Ln, is not enough to induce diastolic dysfunction. Instead, only the concomitant presence of other significant comorbidities, as in ZSF1Ob, prompted HFpEF. Several studies have supported this finding by showing the severity of cardiac

and vascular injuries imposed by hypertension in obese or diabetic patients when compared with hypertension *per se* [66-69].

The HFpEF presentation observed in this metabolic risk model also shares features with clinical presentation of this syndrome. Systolic function, evaluated by CI and EF, was preserved in all groups. Regarding diastolic function, the ZSF1Ob rats presented significant diastolic abnormalities as demonstrated by echocardiography evaluation, mainly and increased myocardial stiffness that compromises a proper ventricular filling. Previous studies from our groups showed that the relaxation time constant $\sigma$ is prolonged in ZSF1Ob, denoting also impaired relaxation [57]. Additionally, the obese group displayed dilated left atrium, lung congestion and increased arterial elastance, contributing to a worse ventricle-vascular coupling, a well establish cause of HFpEF [70]. All these results support the idea of ZSF1Ob as a good animal model of HFpEF.

The current animal model differs from previous experimental HFpEF models, which largely overlooked metabolic risk as they were carried out in old, hypertensive dogs [71, 72] or in Dahl salt sensitive hypertensive rats [73]. ZSF1Ob however closely resembles clinical HFpEF where metabolic risk is highly prevalent as evident from numerous HFpEF registries or large outcome trials [74-76]. HFpEF is a complex disorder that alters cardiac structure and function. Comorbidities commonly adjacent to this pathology, such as obesity, hypertension and diabetes mellitus, are associated with endothelial dysfunction [11, 51]. As a result, patients with HFpEF have an impaired NO response, elevated levels of vasoconstrictors and increased expression of adhesion molecules. Endothelium acquires a chronic inflammatory and pro-thrombotic state where vasodilatation is compromised [32, 36]. Therefore, endothelial dysfunction may be a critical early target for the prevention of HFpEF, since that treatment options are still limited.

## 2. Endothelial dysfunction and oxidative stress

Supplementary data related to vascular function demonstrate that ZSF1Ob animal's aortas are less reactive. Furthermore, ZSF1Ob aortas are the largest and the thickest. In this group, besides the high passive tension, which indicates vascular stiffness, we also observed impairment of relaxation after incubation with a vasodilator substance. Altogether these data suggest endothelial dysfunction. Our results are in agreement with previous studies showing precisely that aortic rings in obese rats had a vasoconstrictive response [77]. Interestingly, Ang 1-7 circulating levels are increased in an attempt to compensate for the increase stiffness of ZSF1Ob arteries.

Many HFpEF-associated comorbidities are known to induce cardiac and systemic ROS production, which further contributes to oxidative stress [78]. In our study the expression of NADPH oxidases, NOX4 and NOX2, with opposite functions, was in agreement with other studies where NOX 2 upregulation in cardiac tissue was observed [79]. In ZSF1Ob, NOX2 upregulation versus NOX4 downregulation clearly imbalances ROS production/protective mechanisms, promoting an oxidative stress environment.

It is well known that DM-induced oxidative stress contributes to the formation of AGEs in cardiomyocytes [80]. Both ZSF1 groups demonstrated significantly higher levels of RAGEs and a small tendency to increase CML in ZSF1Ob. Others studies found similar results of RAGE levels in diabetic hearts [81]. These results were not confirmed by immunohistochemistry analysis of myocardial tissue. Thus this important signaling pathway needs to be clarified in subsequent studies.

Increased systemic inflammation is a hallmark of all the comorbidities associated to this animal model. Interestingly, ZSF1Ob showed a slight tendency to have lower levels of several inflammatory mediators. This phenomenon has recently been described as the obesity paradox. This theory believes that obesity can, under certain circumstances actually have a positive effect due to the capacity of lipoproteins to neutralize

lipopolysaccharide derived from intestinal bacterial translocation. The mortality of obese patients with HF is low. This theory has been described as “reverse epidemiology” [82, 83]. So, the obesity presented by ZSF1Ob animals could attenuate the inflammatory effect. Interestingly, WKY displayed the highest levels of the pro-inflammatory Il-6 and TNFα. A possible explanation for this finding is that, WKY being a genetic model of depression, have hyper-responses to stress and display depression-associated abnormalities, like inflammation [84]. In fact, and supporting our results, other studies have been reported similar inflammatory levels [85, 86]. Current studies are being carried out in laboratory to clarify this aspect.

Regarding tissue inflammation, the increase expression of E-selectin and CD45 in ZSF1Ob animals denotes increased levels of inflammation specifically in endothelial cells.

All the above evidences suggest that ZSF1 animals do not display pronounced systemic alterations but present cardiac-tissue and vascular inflammation. Comorbidities stimulated the expression of inflammatory markers in ZSF1Ob hearts, mainly in endothelium, leading to diastolic dysfunction. We can conclude that comorbidities-induced inflammation and oxidative stress seem to be the hallmark of diastolic dysfunction and progression towards HFpEF.

# Part 6

## Conclusion and future perspectives

*“Somewhere, something incredible is waiting to be known.”*

Carl Sagan

Unfortunately and despite all advances in medicine, HFpEF still remains with no available therapeutic options. Endothelial dysfunction, a state present in HFpEF, seems to be involved in its pathogenesis. An appropriate animal model as ZSF1Ob will certainly help to better understand this syndrome as well as to test new potential therapeutic targets.

Our data clearly show that ZSF1Ob rat presents diastolic dysfunction and HFpEF. Furthermore, both morphometric and metabolic studies already perform in our laboratory confirm the metabolic syndrome state of this animal model, corroborating its cardiometabolic risk, typically associated to HFpEF in the clinical scenario.

We fulfill our goal to evaluate endothelial dysfunction in the ZSF1Ob rat model. Our results evidently showed that ZSF1Ob aortas are predominantly under a rigid and vasoconstriction state. Thus, our data suggest that a dysfunctional endothelium induces an increased vascular stiffness and impaired relaxation, with obvious myocardial deleterious consequences.

We showed that cardiac endothelial cells from ZSF1Ob animals are under a state of endothelial inflammation, which suggests that comorbidities accumulated by these animals stimulate the expression of some important inflammatory markers, culminating in endothelial dysfunction.

There seems to be no doubt that endothelial dysfunction is related to HFpEF development. In this context, it is important to note that endothelium is no longer viewed as a physical barrier that basically separates blood from the vessel wall. In fact, over the years endothelial dysfunction has been associated with several diseases, including HFpEF. Important advances have been made to better understand this relationship but future studies will enable the development of new therapeutic targets with a possible cure.

In the future we aim to complete our studies evaluating ROS systemically by measuring plasma levels of malondialdehyde (MDA) and urinary levels of 8-hydroxydeoxyguanosine (8-OHdG), both markers of oxidative DNA damage. We also want to detect ROS in cultured tissue with a dihydroethidium (DHE) oxidative fluorescent probe. Additionally we pretend to

measure NO levels in heart tissue as well as in vessels supernatant after functional studies.

# Part 7

## References

*“Research is what I'm doing when I don't know what I'm doing.”*

Wernher Von Braun

1. Dhingra, A., et al., *Epidemiology of heart failure with preserved ejection fraction.* Curr Heart Fail Rep, 2014. **11**(4): p. 354-65.
2. Dorhout Mees, E.J., *Diastolic heart failure: a confusing concept.* Heart Fail Rev, 2013. **18**(4): p. 503-9.
3. Heineke, J. and J.D. Molkentin, *Regulation of cardiac hypertrophy by intracellular signalling pathways.* Nat Rev Mol Cell Biol, 2006. **7**(8): p. 589-600.
4. Roger, V.L., *Epidemiology of heart failure.* Circ Res, 2013. **113**(6): p. 646-59.
5. Ponikowski, P., et al., *Heart failure: preventing disease and death worldwide.* ESC Heart Failure, 2014. **1**: p. 4-25.
6. Nichols, M., et al., *Cardiovascular disease in Europe: epidemiological update.* Eur Heart J, 2013. **34**(39): p. 3028-34.
7. Andersen, M.J. and B.A. Borlaug, *Heart failure with preserved ejection fraction: current understandings and challenges.* Curr Cardiol Rep, 2014. **16**(7): p. 501.
8. Aziz, F., et al., *Heart failure with preserved EF: a bird eye view.* JNMA J Nepal Med Assoc, 2013. **52**(190): p. 405-12.
9. Yancy, C.W., et al., *2013 ACCF/AHA guideline for the management of heart failure: a report of the American College of Cardiology Foundation/American Heart Association Task Force on Practice Guidelines.* J Am Coll Cardiol, 2013. **62**(16): p. e147-239.
10. Komamura, K., *Similarities and Differences between the Pathogenesis and Pathophysiology of Diastolic and Systolic Heart Failure.* Cardiology Research and Practice, 2013. **2013**: p. 6.
11. van Heerebeek, L. and W.J. Paulus, *Impact of Comorbidities on Myocardial Remodeling and Dysfunction In Heart Failure with Preserved Ejection Fraction.* SOJ Pharmacy & Pharmaceutical Sciences, 2014. **1**(2): p. 20.
12. Oktay, A.A., J.D. Rich, and S.J. Shah, *The emerging epidemic of heart failure with preserved ejection fraction.* Curr Heart Fail Rep, 2013. **10**(4): p. 401-10.
13. Glezeva, N. and J.A. Baugh, *Role of inflammation in the pathogenesis of heart failure with preserved ejection fraction and its potential as a therapeutic target.* Heart Fail Rev, 2014. **19**(5): p. 681-94.
14. Hummel, S.L. and D.W. Kitzman, *Update on heart failure with preserved ejection fraction.* Curr Cardiovasc Risk Rep, 2013. **7**(6): p. 495-502.
15. Bhuiyan, T. and M.S. Maurer, *Heart Failure with Preserved Ejection Fraction: Persistent Diagnosis, Therapeutic Enigma.* Curr Cardiovasc Risk Rep, 2011. **5**(5): p. 440-449.
16. Wang, Z., et al., *Vascular endothelial function of patients with stable coronary artery disease.* Pak J Med Sci, 2015. **31**(3): p. 538-42.
17. Leite-Moreira, A.F., *Current perspectives in diastolic dysfunction and diastolic heart failure.* Heart, 2006. **92**(5): p. 712-8.
18. Borlaug, B.A., *The pathophysiology of heart failure with preserved ejection fraction.* Nat Rev Cardiol, 2014. **11**(9): p. 507-15.
19. Barry, S.P., S.M. Davidson, and P.A. Townsend, *Molecular regulation of cardiac hypertrophy.* Int J Biochem Cell Biol, 2008. **40**(10): p. 2023-39.
20. Heusch, G., et al., *Cardiovascular remodelling in coronary artery disease and heart failure.* Lancet, 2014. **383**(9932): p. 1933-43.
21. Asrar Ul Haq, M., et al., *Heart failure with preserved ejection fraction - unwinding the diagnosis mystique.* Am J Cardiovasc Dis, 2014. **4**(3): p. 100-13.
22. Borlaug, B.A. and W.J. Paulus, *Heart failure with preserved ejection fraction: pathophysiology, diagnosis, and treatment.* Eur Heart J, 2011. **32**(6): p. 670-9.
23. Palau, P., et al., *Physical therapy in heart failure with preserved ejection fraction: A systematic review.* Eur J Prev Cardiol, 2014.

24. Scantlebury, D.C. and B.A. Borlaug, *Why are women more likely than men to develop heart failure with preserved ejection fraction?* Curr Opin Cardiol., 2011. **26**(6): p. 562-8.
25. Mentz, R.J. and G.M. Felker, *Noncardiac comorbidities and acute heart failure patients.* Heart Fail Clin, 2013. **9**(3): p. 359-67, vii.
26. Falcao-Pires, I., et al., *Diabetes mellitus worsens diastolic left ventricular dysfunction in aortic stenosis through altered myocardial structure and cardiomyocyte stiffness.* Circulation, 2011. **124**(10): p. 1151-9.
27. Susic, D., *Cross-link breakers as a new therapeutic approach to cardiovascular disease.* Biochemical Society Transactions, 2007. **35**(5): p. 853-6.
28. Leung, M., V. Phan, and D.Y. Leung, *Endothelial function and left ventricular diastolic functional reserve in type 2 diabetes mellitus.* Open Heart, 2014. **1**(1): p. e000113.
29. Hansson, G.K., *Inflammation, atherosclerosis, and coronary artery disease.* N Engl J Med, 2005. **352**(16): p. 1685-95.
30. Hadi, H.A., C.S. Carr, and J. Al Suwaidi, *Endothelial dysfunction: cardiovascular risk factors, therapy, and outcome.* Vasc Health Risk Manag, 2005. **1**(3): p. 183-98.
31. Yang, O., J. Li, and J. Kong, *The Endothelium as a Target for the Treatment of Heart Failure.* Cell Biochem Biophys, 2015.
32. Marti, C.N., et al., *Endothelial dysfunction, arterial stiffness, and heart failure.* J Am Coll Cardiol, 2012. **60**(16): p. 1455-69.
33. Lam, C.S. and D.L. Brutsaert, *Endothelial dysfunction: a pathophysiologic factor in heart failure with preserved ejection fraction.* J Am Coll Cardiol, 2012. **60**(18): p. 1787-9.
34. Tomiyama, H. and A. Yamashina, *Vascular Dysfunction: A Key Player in Chronic Cardio-renal Syndrome.* Intern Med, 2015. **54**(12): p. 1465-72.
35. Hartge, M.M., T. Unger, and U. Kintscher, *The endothelium and vascular inflammation in diabetes.* Diab Vasc Dis Res, 2007. **4**(2): p. 84-8.
36. Endemann, D.H. and E.L. Schiffrin, *Endothelial dysfunction.* J Am Soc Nephrol, 2004. **15**(8): p. 1983-92.
37. Patel, S.J., et al., *The inflammatory response to double stranded DNA in endothelial cells is mediated by NFkappaB and TNFalpha.* PLoS One, 2011. **6**(5): p. e19910.
38. Tschope, C. and S. Van Linthout, *New insights in (inter)cellular mechanisms by heart failure with preserved ejection fraction.* Curr Heart Fail Rep, 2014. **11**(4): p. 436-44.
39. Mather, K.J., *The vascular endothelium in diabetes--a therapeutic target?* Rev Endocr Metab Disord, 2013. **14**(1): p. 87-99.
40. Raij, L., *Nitric oxide in the pathogenesis of cardiac disease.* J Clin Hypertens (Greenwich), 2006. **8**(12 Suppl 4): p. 30-9.
41. Tousoulis, D., et al., *The role of nitric oxide on endothelial function.* Curr Vasc Pharmacol, 2012. **10**(1): p. 4-18.
42. Khazaei, M., F. Moien-Afshari, and I. Laher, *Vascular endothelial function in health and diseases.* Pathophysiology, 2008. **15**(1): p. 49-67.
43. Taylor, A.L., *Nitric oxide modulation as a therapeutic strategy in heart failure.* Heart Fail Clin, 2012. **8**(2): p. 255-72.
44. Deanfield, J.E., J.P. Halcox, and T.J. Rabelink, *Endothelial function and dysfunction: testing and clinical relevance.* Circulation, 2007. **115**(10): p. 1285-95.
45. Reriani, M.K., L.O. Lerman, and A. Lerman, *Endothelial function as a functional expression of cardiovascular risk factors.* Biomark Med, 2010. **4**(3): p. 351-60.

46. Avogaro, A., et al., *Endothelial dysfunction in diabetes: the role of reparatory mechanisms.* Diabetes Care, 2011. **34 Suppl 2**: p. S285-90.
47. Akiyama, E., et al., *Incremental prognostic significance of peripheral endothelial dysfunction in patients with heart failure with normal left ventricular ejection fraction.* J Am Coll Cardiol, 2012. **60**(18): p. 1778-86.
48. Versari, D., et al., *Endothelial dysfunction as a target for prevention of cardiovascular disease.* Diabetes Care, 2009. **32 Suppl 2**: p. S314-21.
49. Rajendran, P., et al., *The vascular endothelium and human diseases.* Int J Biol Sci, 2013. **9**(10): p. 1057-69.
50. Prieto, D., C. Contreras, and A. Sanchez, *Endothelial dysfunction, obesity and insulin resistance.* Curr Vasc Pharmacol, 2014. **12**(3): p. 412-26.
51. Paulus, W.J. and C. Tschope, *A novel paradigm for heart failure with preserved ejection fraction: comorbidities drive myocardial dysfunction and remodeling through coronary microvascular endothelial inflammation.* J Am Coll Cardiol, 2013. **62**(4): p. 263-71.
52. Trepels, T., A.M. Zeiher, and S. Fichtlscherer, *The endothelium and inflammation.* Endothelium, 2006. **13**(6): p. 423-9.
53. van Heerebeek, L., et al., *Low myocardial protein kinase G activity in heart failure with preserved ejection fraction.* Circulation, 2012. **126**(7): p. 830-9.
54. Badenhorst, D., et al., *Cross-linking influences the impact of quantitative changes in myocardial collagen on cardiac stiffness and remodelling in hypertension in rats.* Cardiovasc Res, 2003. **57**(3): p. 632-41.
55. Srinivasan, K. and P. Ramarao, *Animal models in type 2 diabetes research: an overview.* Indian J Med Res, 2007. **125**(3): p. 451-72.
56. King, J.F.A., *The use of animal models in diabetes research.* British Journal of Phamacology 2012. **166**: p. 877–894.
57. Hamdani, N., et al., *Myocardial titin hypophosphorylation importantly contributes to heart failure with preserved ejection fraction in a rat metabolic risk model.* Circ Heart Fail, 2013. **6**(6): p. 1239-49.
58. Tofovic, S.P., et al., *2-Hydroxyestradiol attenuates renal disease in chronic puromycin aminonucleoside nephropathy.* J Am Soc Nephrol, 2002. **13**(11): p. 2737-47.
59. Bilan, V.P., et al., *Diabetic nephropathy and long-term treatment effects of rosiglitazone and enalapril in obese ZSF1 rats.* J Endocrinol, 2011. **210**(3): p. 293-308.
60. Tofovic, S.P., et al., *Long-term caffeine consumption exacerbates renal failure in obese, diabetic, ZSF1 (fa-fa(cp)) rats.* Kidney Int, 2002. **61**(4): p. 1433-44.
61. Tofovic, S.P., et al., *Renal function and structure in diabetic, hypertensive, obese ZDFxSHHF-hybrid rats.* Ren Fail, 2000. **22**(4): p. 387-406.
62. Joshi, D., et al., *TRC4186, a novel AGE-breaker, improves diabetic cardiomyopathy and nephropathy in Ob-ZSF1 model of type 2 diabetes.* J Cardiovasc Pharmacol, 2009. **54**(1): p. 72-81.
63. Rafikova, O., E.M. Salah, and S.P. Tofovic, *Renal and metabolic effects of tempol in obese ZSF1 rats--distinct role for superoxide and hydrogen peroxide in diabetic renal injury.* Metabolism, 2008. **57**(10): p. 1434-44.
64. Zambad, S.P., et al., *TRC150094 attenuates progression of nontraditional cardiovascular risk factors associated with obesity and type 2 diabetes in obese ZSF1 rats.* Diabetes Metab Syndr Obes, 2011. **4**: p. 5-16.
65. Falcao-Pires, I., et al., *Apelin decreases myocardial injury and improves right ventricular function in monocrotaline-induced pulmonary hypertension.* Am J Physiol Heart Circ Physiol, 2009. **296**(6): p. H2007-14.
66. Virdis, A., et al., *Microvascular endothelial dysfunction in obesity and hypertension.* Curr Pharm Des, 2013. **19**(13): p. 2382-9.

67. Hadi, H.A. and J.A. Suwaidi, *Endothelial dysfunction in diabetes mellitus.* Vasc Health Risk Manag, 2007. **3**(6): p. 853-76.
68. Varughese, G.I., *The impact of diabetes mellitus on endothelial dysfunction.* South Med J, 2007. **100**(2): p. 128-9.
69. Dandona, P., A. Chaudhuri, and A. Aljada, *Endothelial dysfunction and hypertension in diabetes mellitus.* Med Clin North Am, 2004. **88**(4): p. 911-31, x-xi.
70. Borlaug, B.A. and D.A. Kass, *Ventricular-vascular interaction in heart failure.* Heart Fail Clin, 2008. **4**(1): p. 23-36.
71. Bishu, K., et al., *Sildenafil and B-type natriuretic peptide acutely phosphorylate titin and improve diastolic distensibility in vivo.* Circulation, 2011. **124**(25): p. 2882-91.
72. Hamdani, N., et al., *Deranged myofilament phosphorylation and function in experimental heart failure with preserved ejection fraction.* Cardiovasc Res, 2013. **97**(3): p. 464-71.
73. Westermann, D., et al., *Enhancement of the endothelial NO synthase attenuates experimental diastolic heart failure.* Basic Res Cardiol, 2009. **104**(5): p. 499-509.
74. Ather, S., et al., *Impact of noncardiac comorbidities on morbidity and mortality in a predominantly male population with heart failure and preserved versus reduced ejection fraction.* J Am Coll Cardiol, 2012. **59**(11): p. 998-1005.
75. McMurray, J.J., et al., *Heart failure with preserved ejection fraction: clinical characteristics of 4133 patients enrolled in the I-PRESERVE trial.* Eur J Heart Fail, 2008. **10**(2): p. 149-56.
76. Edelmann, F., et al., *Contribution of comorbidities to functional impairment is higher in heart failure with preserved than with reduced ejection fraction.* Clin Res Cardiol, 2011. **100**(9): p. 755-64.
77. Chinen, I., et al., *Vascular lipotoxicity: endothelial dysfunction via fatty-acid-induced reactive oxygen species overproduction in obese Zucker diabetic fatty rats.* Endocrinology, 2007. **148**(1): p. 160-5.
78. Raza, H., A. John, and F.C. Howarth, *Alterations in glutathione redox metabolism, oxidative stress, and mitochondrial function in the left ventricle of elderly Zucker diabetic fatty rat heart.* Int J Mol Sci, 2012. **13**(12): p. 16241-54.
79. Murdoch, C.E., et al., *Endothelial NADPH oxidase-2 promotes interstitial cardiac fibrosis and diastolic dysfunction through proinflammatory effects and endothelial-mesenchymal transition.* J Am Coll Cardiol, 2014. **63**(24): p. 2734-41.
80. Hegab, Z., et al., *Role of advanced glycation end products in cardiovascular disease.* World J Cardiol, 2012. **4**(4): p. 90-102.
81. Aragno, M., et al., *Oxidative stress-dependent impairment of cardiac-specific transcription factors in experimental diabetes.* Endocrinology, 2006. **147**(12): p. 5967-74.
82. Bosello, O. and M.P. Donataccio, *Obesity paradox.* Eat Weight Disord, 2013. **18**(4): p. 447-8.
83. Hainer, V. and I. Aldhoon-Hainerova, *Obesity paradox does exist.* Diabetes Care, 2013. **36 Suppl 2**: p. S276-81.
84. Will, C.C., F. Aird, and E.E. Redei, *Selectively bred Wistar-Kyoto rats: an animal model of depression and hyper-responsiveness to antidepressants.* Mol Psychiatry, 2003. **8**(11): p. 925-32.
85. Bernard, C., et al., *Resistance to endotoxin shock in spontaneously hypertensive rats.* Hypertension, 1998. **31**(6): p. 1350-6.
86. Lourenco, A.P., et al., *A Western-type diet attenuates pulmonary hypertension with heart failure and cardiac cachexia in rats.* J Nutr, 2011. **141**(11): p. 1954-60.

· U C ·

UNIVERSIDADE DE COIMBRA